TIME SERIES PHOTOMETRY OF THE SYMBIOTIC STAR V1835 AQL AND NEW VARIABLE STARS IN AQUILA

Robert Caddy

A Thesis

Submitted to the Graduate College of Bowling Green
State University in partial fulfillment of
the requirements for the degree of

MASTER OF SCIENCE

May 2018

Committee:

Andrew Layden, Advisor

John Laird

Dale Smith

ABSTRACT

Andrew Layden, Advisor

Photographic plates in the Harvard collection show the star V1835 Aql brightening by a factor of 100 in flux over four years starting in 1899, remaining at maximum for four years, then declining below the depth of the plates [1]. This nova-like behavior is very atypical for most variable stars and as a result there has been much debate over the exact nature of V1835 Aql. This debate was ended by the discovery of a Raman scattered emission line at 6824 Å, which is unique to symbiotic binaries and unequivocally identifies V1835 Aql as a symbiotic star [2]. Our research hopes to expand upon our knowledge of V1835 Aql through analysis of five years worth of multi-band optical time-series photometry. From this we have found the period of this star to be 419 days. This long period confirms that V1835 Aql is a symbiotic star and not its closer orbiting cousin, a cataclysmic variable. We have also determined the properties of all the other variable star candidates near V1835 Aql, of which there are 31.

To my parents for their unequivocating love and support

TABLE OF CONTENTS

LIST OF FIGURES

LIST OF TABLES

CHAPTER 1
INTRODUCTION

Studying stars late in their life is critical for advancing our knowledge of physics and is one of the few places in the universe where we can study the most extreme phenomena. These objects represent some of the most extreme and interesting physics in our universe and often this kind of physics cannot be replicated in a laboratory. The mass of a star is crucial to its late-stage development. During the main sequence stage it fuses hydrogen to helium and once it builds up a helium core it begins to climb the red giant branch. After core densities and temperatures get high enough, helium fusion begins and a carbon core starts to build up. The most massive stars will continue this process until they have a roughly earth-sized core of iron.

Stars with masses up to about 15 $M_{\odot}$ will stop fusing at an earlier point and become white dwarf stars. White dwarfs are made of some combination of helium, carbon, oxygen, and neon (depending on the mass of the progenitor star) and, instead of being supported by radiation and thermal pressure from fusion as in main sequence stars, they are supported by electron degeneracy pressure. There is a maximum mass that electron degeneracy pressure can support and this is called the Chandrasekhar Limit, roughly 1.4 $M_{\odot}$. The mass that will not become part of the white dwarf is blown off through thermal pulses and stellar wind during the late stages of the star's evolution. Stars with initial masses that are very approximately between 15 $M_{\odot}$ and 18 $M_{\odot}$ become neutron stars. These stars are limited to 1.5-3 $M_{\odot}$ by the Tolman-Oppenheimer-Volkoff (TOV) Limit. Above about 18 $M_{\odot}$ stars will core collapse and become black holes[3].

1.1 Variable Stars

Any star whose luminosity or color changes as a function of time is considered a variable star. While all stars are variable to some degree the variability is typically either extremely small or only noticeable during geologic time scales. Stars that do vary significantly on human time scales are typically very young, highly evolved, very massive, or lie within the instability strip. These variations can be generally classified as extrinsic or intrinsic.

1.1.1 Extrinsic Variables

Extrinsic variables vary by two main mechanisms, eclipses and rotation. Eclipsing variables are binary systems whose orbital plane is inclined about 90° towards the earth so we see the emitted light dip as one star (or planet) occults the other star. These orbiting stars can be so close that they share a common envelope or so far apart that they take decades to orbit each other. Rotating variables are stars that have hot or cold spots, tidal distortion, or a combination thereof. As the variable rotates, different areas of the star come into view, causing variations in the brightness (and sometimes color) of the rotating variable with one to two brightness cycles per rotation.

Ellipsoidal variables are a sub-group of rotating variables that vary not due to rotation of the star about its axis but by how it moves through its orbit with a companion star. Since the variability of ellipsoidal variables depends on the orbital period, their light curves are extremely regular, unlike many intrinsic variables. This does not mean that their light curves are simple though; Often they will have two dips in brightness per orbit, one of which can be significantly greater than the other. Pairing this with a full or partial eclipse every orbit and their light curves can be quite complex.

These sources of variability in ellipsoidal variables depend on the geometry of the system and therefore the angle at which we view the system can significantly affect what we see (to the point where they can look quite different). For example, if there is a binary system of two similarly sized stars then when the system is viewed at a low inclination (face on) then the system will appear to have an unvarying brightness, if the system is viewed at a high inclination (edge on) then there will be significant variation due to each star eclipsing the other, and in the intermediate case there will be sinusoidal variation due to the tidal distortion of one or both stars.

1.1.2 Intrinsic Variables

There are two main types of intrinsic variables: pulsating and explosive (sometimes called cataclysmic). Pulsating variables vary due to physical pulsations in the size and temperature of the star and come in two general types: shorter period variables, such as RR Lyrae stars with periods of 0.2-1 day or Cepheid stars with periods of 2-100 days, and Long Period Variables (LPV) with longer periods, such as Mira type stars with periods of 100 days or more. Before stars become white dwarfs, neutron stars, or black holes, and during the periods when they are burning elements heavier than hydrogen, they are often less stable than they are during the main sequence stage. This instability often leads to significant variability in the brightness of the stars, caused either by changing in size or temperature. The Stefan-Boltzmann law states that the luminosity of a star is dependent on its radius and temperature as follows:

$$L = 4\pi R^2 \sigma_{SB} T_e^4 \tag{1.1}$$

where L is the luminosity, R is the radius of the star, σ_{SB} is the Stefan-Boltzmann constant, and T_e is the effective surface temperature. Stars that vary in brightness by changing one or both of R and T_e are called intrinsic variables.

Long Period (Pulsating) Variables

Long Period Variables (LPVs) are red giant stars, with a spectral type of K or M, that pulsate radially, changing their size and temperature, and thus brightness. There are three primary types of LPV's: Mira, semi-regular, and irregular. Mira variables have periods longer than 100 days and have large amplitudes, from 2.5 to 11.0 magnitudes, with little to no changes from period to period. Semi-regular variables have small, quasi-regular amplitudes with multiple overlapping periods. Irregular variables typically have small amplitudes with very little regularity in either amplitude or period, even less regularity than semi-regular variables[4].

Explosive Variables

Explosive variables are stars that vary in brightness due to thermonuclear events either on the surface or within the star. Typically these stars are in close binaries where a larger, cooler star transfers mass to a small, hot, compact object such as a white dwarf, neutron star, or black hole that is surrounded by an accretion disk. This mass transfer can occur through a variety of mechanisms including stellar wind and Roche lobe overflow[4]. There are several different types of explosive variables including supernovae, novae, recurrent novae, dwarf novae, and symbiotic novae.

Supernovae show a sudden brightening on the order of 20 mag over a few days to a week and are the result of a catastrophic stellar explosion. There are several types of supernovae. Some are caused by the core collapse of evolved, high-mass stars as they become a neutron star or black hole. Type Ia supernovae, however, are believed to be caused by a thermonuclear runaway reaction in a white dwarf star. This often occurs through accretion in tight binary systems. The white dwarf gains mass until it exceeds the Chandrasekhar limit and explodes in a Type Ia supernova.

Novae occur in close binary systems with an accreting white dwarf whose mass is below the Chandrasekhar limit. Explosive nuclear burning of accreted material on the surface of the white dwarf causes the system to brighten 7 to 16 magnitudes over the period of one to several hundred days. After the initial brightening event the star slowly fades back to quiescence over an interval of typically months to decades. Recurrent novae are simply systems that have been observed to experience a nova event multiple times, sometimes with regular outbursts.

Dwarf Novae occur in close binary systems with a red dwarf and a white dwarf with an accretion disk. They regularly brighten by 2 to 6 magnitudes due to instabilities within the accretion disk that drain mass from the disk onto the white dwarf and the rapid build up of mass causes a short burst of thermonuclear fusion on the surface of the white dwarf. There are several subtypes of dwarf novae but none of their nova events last longer than 20 days.

Novae and Dwarf Novae are both examples of cataclysmic variables, stars that vary suddenly and enormously due to thermonuclear runaway or disk instabilities. These systems are close binaries with a compact star orbiting very close to the primary; typical orbital periods range from minutes to a few days at most. During quiescence these binaries can be detected via eclipses or flickering of the accretion stream.

1.2 Symbiotic Stars

Symbiotic Stars (SySt) are binary systems consisting of a red giant and a hot, compact object, typically a white dwarf. SySts are important because they typically have an actively accreting white dwarf that has the potential to exceed the Chandrasekhar Limit and become a Type Ia supernova[5, 6]. These outbursts are important cosmological distance indicators. There are currently at least 188 known SySts in the Milky Way and Local Group[7]. The light curves of several SySts are shown for reference in Figures 1.1-1.4. Symbiotic stars typically exhibit nova-like events where they will remain at maximum for several years to decades before returning to quiescence over the period of a few years to a few decades.

Figure 1.1 shows the light curve of the well-studied SySt RR Telescopii from its discovery at outburst in 1944 to 2004 as it slowly returns to quiescence, as observed in visual magnitudes by observers from the American Association of Variable Star Observers (AAVSO). Remaining at maximum for several years instead of immediately dimming after reaching maximum makes SySts unique amongst explosive variables. Figure 1.2 shows the phased light curve for RR Tel. Instead of plotting magnitude vs. time the phased light curve shows magnitude vs. the phase of the orbit where the orbital period is found from the photometric data using a Fast Fourier Transform. This allows a much clearer look at the orbital characteristics of the system; in the case of RR Tel the phased light curve is generated from just a small sub-set of the data to avoid the large changes in magnitude that occurred post-outburst.

SySts come in two types, S-type (Figure 1.3) and D-type (Figure 1.4) [8]. S-type SySt's have orbital periods from 200-2000 days with orbital distances of 1-3 AU; in addition, they also have a compact, dense nebula surrounding them. D-type SySt's have orbital periods that are 10 years or longer with orbital distances of around 20 AU; in addition, they also have an extended, dusty, tenuous nebula surrounding them which is often detectable in the far IR. In both types of SySts the giant star can be intrinsically variable, sometimes to the point where its intrinsic variability overpowers the ellipsoidal variations, which can greatly complicate determining the orbital period. These long orbital periods and distances are what differentiate SySts from their closer-orbiting cousins, cataclysmic variables (CV), which have orbital periods on the order of minutes to hours. The primary method of mass transfer in a SySt is transfer through stellar wind whereas cataclysmic variables accrete primarily through Roche lobe overflow.

One feature that makes SySt's unique is emission lines at 6825 Å and 7082 Å. These emission lines are caused by the quintuply ionized oxygen (O VI) doublet at 1032 Å and 1038 Å Raman scattering off of cold, neutral hydrogen. Not all SySt's exhibit these lines and the 7082 Å line is often absent, but no other type of star is known to exhibit these specific emission lines. The reason that these lines are only seen in SySt's is that, unlike other similar binaries, SySt's have thick, cool, sometimes dusty, nebulae surrounding both the red giant and the hot compact object. This juxtaposition of incredibly high temperatures in the white dwarf/disk and the cold surrounding medium is what allows quintuply ionized oxygen emissions to scatter off of cold hydrogen with enough regularity to show a noticeable emission line that is a unique identifier of symbiotic stars.

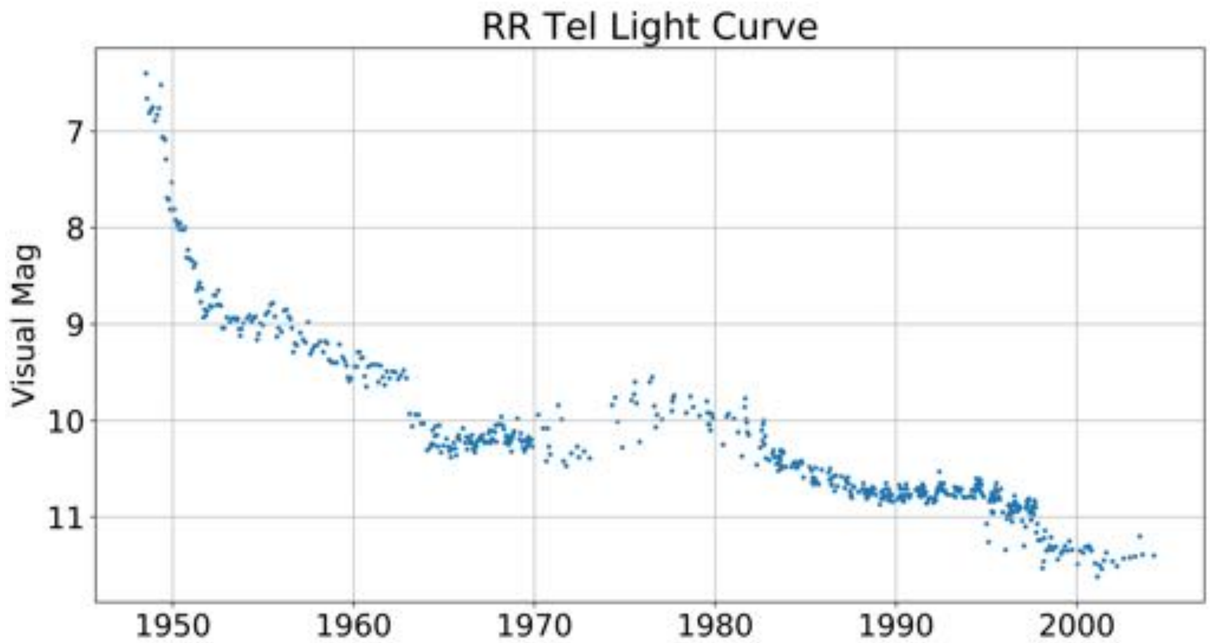

Figure 1.1: Visual light curve of the SySt RR Tel declining from its outburst in 1944 to 2004. Data after 2004 are available in the AAVSO database but the later data are marked as not confirmed by AAVSO and so were omitted from this plot. Source of data: Kafka, S., 2017, Observations from the AAVSO International Database, https://www.aavso.org

1.3 V1835 Aql

V1835 Aql (previously known as NSV 11749) is a recently identified SySt that was originally misidentified as an FU Ori variable or Slow Nova. V1835 Aql was first observed in 1899 with glass plates that now reside in the Harvard College Observatory plate collection and it is detected on a total of 175 plates in that collection[1]. V1835 Aql was originally discovered by W. J. Luyten during the Bruce Proper Motion Survey in the 1930s[1] and additional work was done by David Williams in 2005[1]. V1835 Aql first brightened above the detection threshold in 1899. After this the plates show V1835 Aql brightening by at least

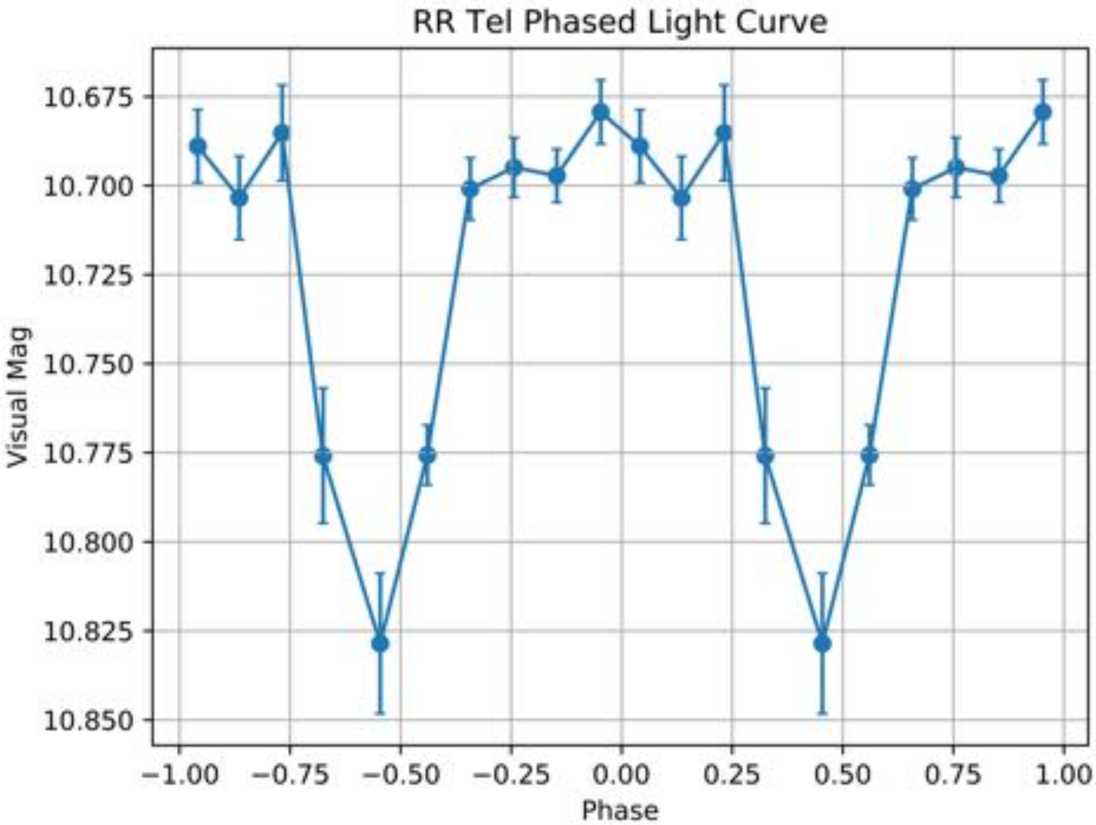

Figure 1.2: Visual phased light curve of the SySt RR Tel with a period of 366 days. Source of data: Kafka, S., 2017, Observations from the AAVSO International Database, https://www.aavso.org

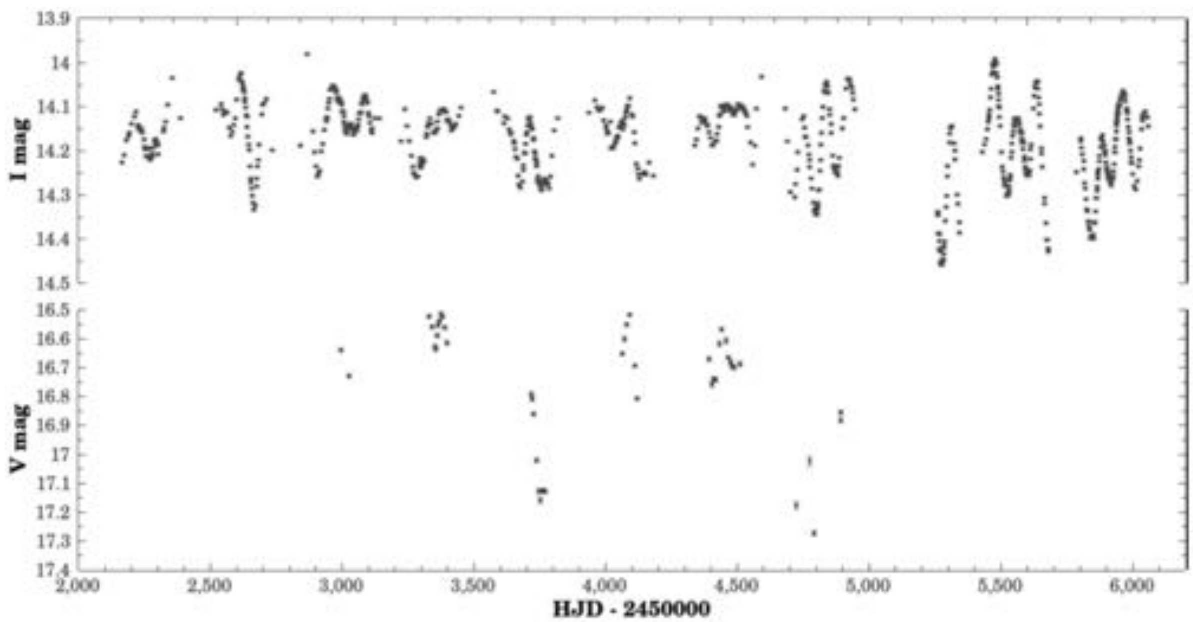

Figure 1.3: I and V band light curves of the SySt LMC-N19. An example of a S-type SySt showing possible ellipsoidal variability with a period of 1000 days. However, the variability is dominated by the much shorter period pulsating variation from the cool component of the system. Figure taken from Angeloni et al. 2014[9]

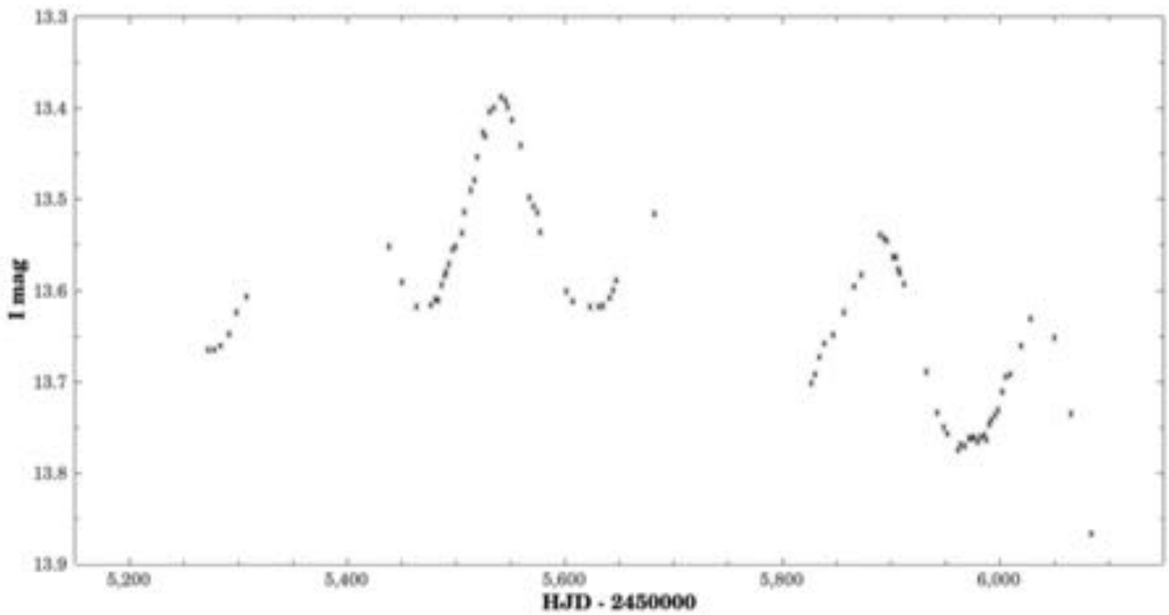

Figure 1.4: *I* band light curve of the SySt LMC-N1. An example of a D-type SySt showing variability due to pulsations of the cool component, a carbon star[9], with a primary period of 171 ± 3 days and a secondary period of 98 ± 2 days. The overall slow rise and fall is a possible long secondary period (LSP). Ellipsoidal variability is not evident. Figure taken from Angeloni et al. 2014[9]

2.5 magnitudes from 1899.5 to 1903.4, remaining at maximum until 1907.6, then dimming until it dropped below the sensitivity of the plates in 1911.6. This behavior is very atypical for most kinds of variable stars and it was suggested by Williams 2005 that V1835 Aql is either a slow nova (novae that take more than 80 days to decay 2-3 magnitudes) or an FU Ori variable (a pre-main sequence star that suddenly changes luminosity and spectral type via mass accretion)[1].

Miller Bertolami et al. (2011) criticized William's suggestion, pointing out that V1835 Aql's brightening event does not fit with either of those types of variables. Slow Novae brighten in a matter of a few weeks then remain at maximum for about a year, after which they slowly decline over several years. FU Ori variables brighten in tens to hundreds of days, then sit at maximum for decades or longer[10]. In contrast V1835 Aql brightened for four years, remained at maximum for four years, then declined for four years. This event is far too long for a Slow Nova and far too short for a FU Ori variable. Instead Miller Bertolami et al. (2011) suggested the alternative hypothesis that V1835 is a born-again red giant (BARG). BARGs are red giant stars that experience a final thermal pulse during their post-asymptotic giant branch evolution[11]. When this happens the star is briefly reborn as a yellow giant[12]. According to stellar evolution theory the two types of pulses experienced by BARG's are late thermal pulses, which last about a century[12], and very late thermal pulses, which last a few years. While this model fits better qualitatively, the time scale for a late thermal pulse is significantly longer than V1835 Aql's outburst, and the time scale for a very late thermal pulse is significantly shorter that V1835 Aql's approximately 12 year long outburst. BARG's also have thick dust shells and Bond & Kasliwal (2012) pointed out the lack of mid-IR lines in the WISE photometry, which indicates that V1835 Aql has no significant dust shell[2].

All of the previous hypotheses were based on data taken from century-old glass plates. Bond & Kasliwal (2012) used modern equipment to inform their research. Their optical and near-infrared spectra of V1835 Aql, which showed a distinct emission line at 6825 Å, which is unique to SySt's, and strong hydrogen lines, which would not be expected in a BARG[2]. These two pieces of information conclusively show that V1835 Aql is not a born-again red giant but a symbiotic binary. However, the relatively small number of observations in the Harvard collection, which are spread across decades, and the spectra taken by Bond & Kasliwal (2012) are insufficient to determine the orbital period or any other interesting properties of V1835 Aql besides the fact that it is a SySt.

V1835 Aql was separately rediscovered during the ChaMPlane project [13], a survey to detect and optically identify x-ray sources such as CVs and X-ray binaries. This led researchers at Bowling Green State University to observe V1835 Aql in V and I bandpass filters for six months during the summer of 2012 to search for short-period variability with periodicity from several minutes to weeks[14]. No short-period variability was found but a clear, slow brightening was observed, indicative of a much longer period than a CV would have[14] and further supporting the interpretation of V1835 as a SySt. This prompted Professor Andrew Layden to continue observing V1835 Aql for the next five years.

In Chapter 2 the details of the observations are given. In Chapter 3 the techniques and software used for image reduction and photometry are described. In Chapter 4 the calibration from instrumental to standard magnitudes are discussed. In Chapter 5 the color-magnitude diagram and reddening are discussed. In Chapter 6 more historical details of V1835 Aql and the findings regarding it are discussed along with discussion of modeling using PHEOBE. Chapter 7 describes the other variables in the field, each with their own subsection.

CHAPTER 2
OBSERVATIONS

2.1 Instruments

Images of V1835 Aql and the surrounding field were taken with Panchromatic Robotic Optical Monitoring and Polarimetry Telescope C1 and C5 (PROMPT C1 and C5, hereafter referred to as P1 and P5) located at the Cerro Tololo Inter-American Observatory in the Chilean Andes (latitude 30:09:55 S, longitude 70:48:52 W). Both telescopes are Ritchey-Chrétien telescopes. P1 has a diameter of 0.6 m and P5 has a diameter of 0.41m. Their CCD's have a gain of 1.5 electrons/adu and readout noise of 13.5 electrons. P1 has a field of view of 24x24 arcminutes and angular resolution of 1.4 arcseconds per pixel. P5 has a field of view of 10x10 arcminutes and angular resolution of 0.59 arcseconds per pixel[15].

2.2 Imaging

Using the Skynet system Professor Layden's group remotely observed V1835 Aql from June 2012 through May 2017 taking images roughly every two weeks except when the star was below the horizon during the months of December and January. During all of the observations, I and V bandpass filters were used. In addition, B and R filters were used from August 2012 to September 2014 (Figure 2.1); all filters are on the the Johnson-Cousins system. A total 127 nights of data was taken. Due to bad weather, poor seeing, tracking problems, and other issues five nights in the V data and nine nights in the I data had to be rejected. The airmass of an observation indicates how much of the atmosphere the telescope had to look through to get an image of the target. Much lower errors can be achieved by imaging targets at airmasses < 1.5. Unfortunately V1835 Aql is not always above the horizon so to avoid having huge gaps in the data images were taken up to an airmass of around 3. A graph showing airmass vs. time for the data can be found in Figure 2.2.

The data were divided into three different sets based on the telescope and CCD used; these data sets are P1_AU, P5_AU, and P5_AA. The P1 and P5 sets were taken with the P1 and P5 telescopes respectively. The AU or AA indicate which CCD was used: Apogee USB/Net and Apogee Alta (as indicated by the FITS header for each image). The data sets were split when the CCD was changed since the different CCDs will have slightly different sensitivities to different wavelengths. This change in sensitivity could potentially induce a systematic error when using the image reduction software since it was not written to handle changes in sensitivity of the CCD. The P5_AU data set is fragmented because of CCD changes and the fluctuating availability of the telescope; for details see Table 2.1. Figure 2.3 shows an example image taken by P1 and Figure 2.4 shows an example of an image taken by P5.

Table 2.1: Data Set Date Ranges

Data set	Date Range
P1_AU	23-June-2016 to 8-November-2016
P5_AU	29-July-2014 & 2-March-2015 to 20-May-2016 & 28-February-2017 to 29-June-2017
P5_AA	24-June-2012 to 12-November-2014

On most nights six different images were taken with two different filters: three 12-second long exposures in I and three 30-second long exposures in V. For a small subset of nights different exposure times and number of images were used to get deeper images or to avoid saturation. For the nights with B and R data typically three 30-second long R exposures and four 60-second long B exposures were taken. Unfortunately these B exposures were typically not long enough to get a reasonable signal-to-noise ratio and so more than half of the nights in B were unusable and were consequently rejected, leaving only 23 nights in B

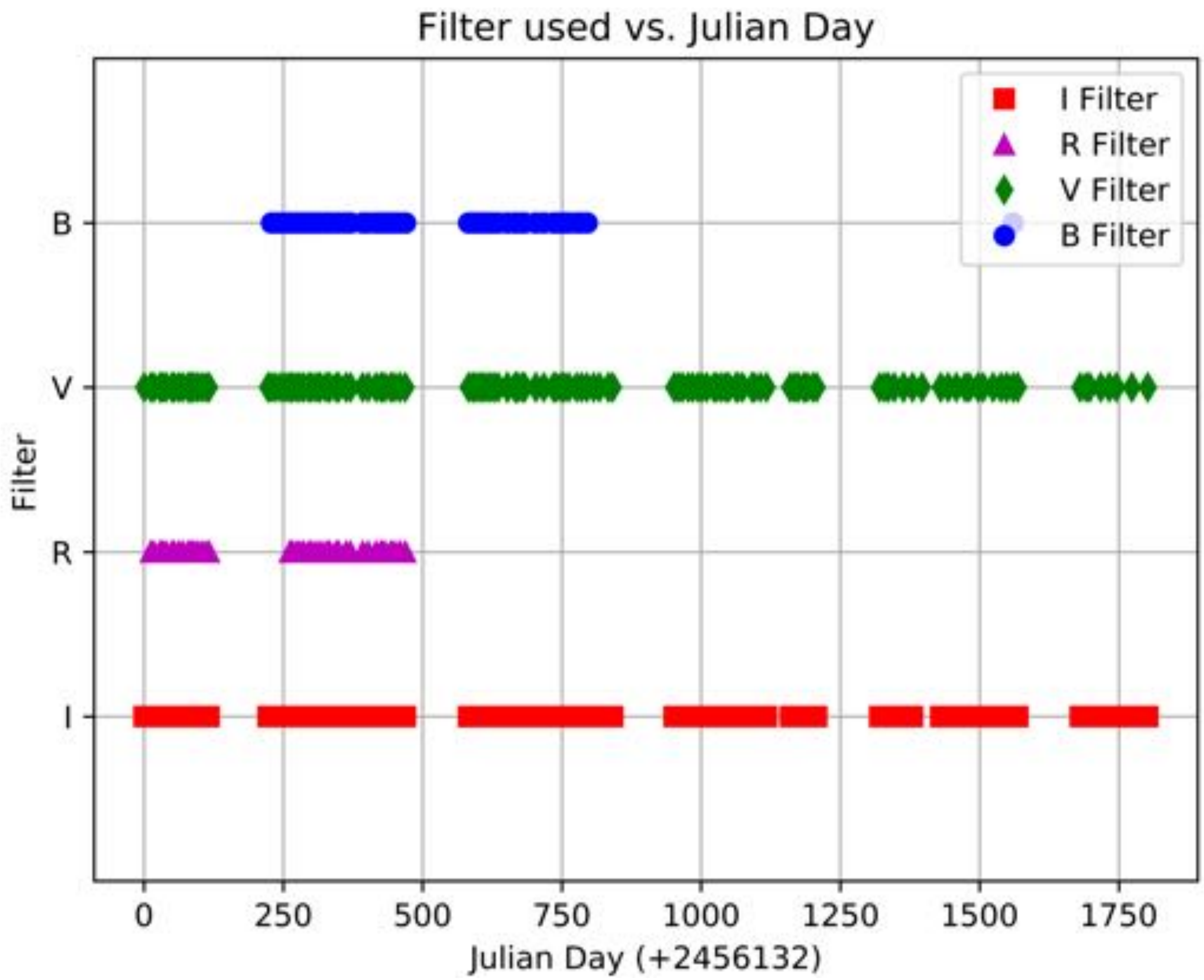

Figure 2.1: Filter used vs. Julian Date. This plot shows which filters were used as a function of time. Note that most of the late B and early R images had to be rejected from the data set due to poor quality. The seasonal gaps are due to Aquila being below the horizon between late November and late February.

and 39 nights in R. The reason that the exposure times on the B images were not increased beyond 60 s is that the telescopes are not actively guided so exposures much longer than 60 s become severely trailed, making them nearly useless for accurate photometry.

If there is a bad pixel on the CCD it is possible that a star could land on that pixel on each image and result in erroneous magnitudes for that star on a particular night. To

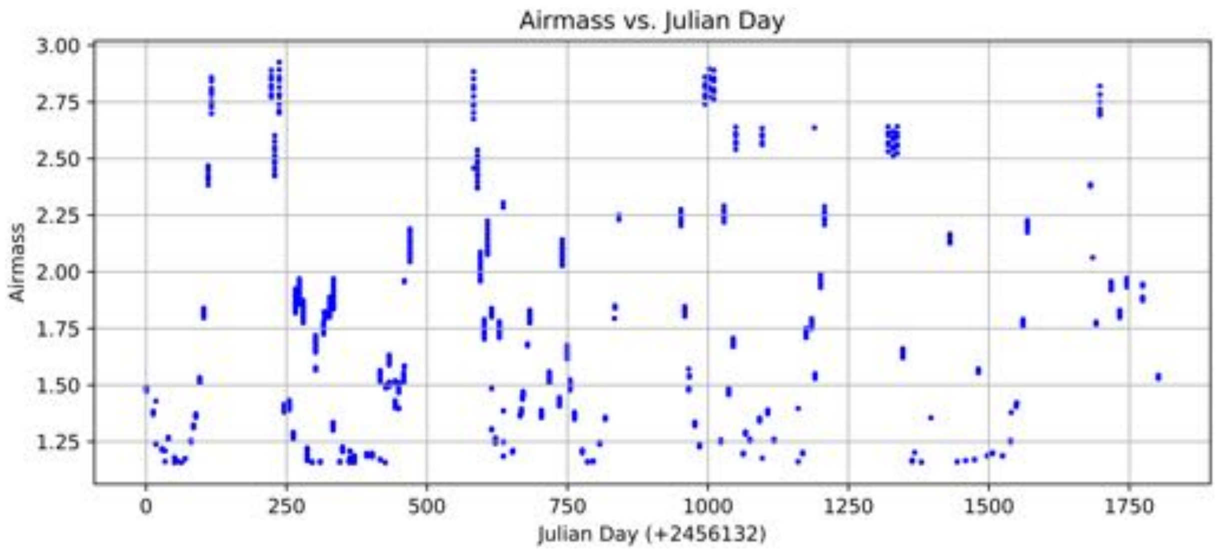

Figure 2.2: Airmass vs. Julian Date. The seasonal gaps and the high airmasses that proceed and succeed each gap are clearly visible. Most of the images were taken with an airmass of < 2. The reason that the higher airmass (> 2) images appear in columns is that when the target is at a high airmass, the airmass can change significantly over a sequence of observations, leading to those distinctive columns for each night. If the airmass changes slowly throughout the observations, as it does when the target is far from the horizon, then all the images from that observation will appear very close in airmass to each other instead of in a long column.

avoid this, one of two techniques was used on each night, depending on the capabilities of the Skynet system. The preferred method is called dithering, where each time a new exposure is started the telescope moves by a tiny amount (5 arcseconds in our case). During most of our observation time this could not be done because the Skynet and Terminator systems used to control the telescope did not have this functionality. Because of this most of the data use interleaved filters, where images are taken in alternating filters so that the natural small movements of the telescope keep a given star off of a bad pixel for more than a single image.

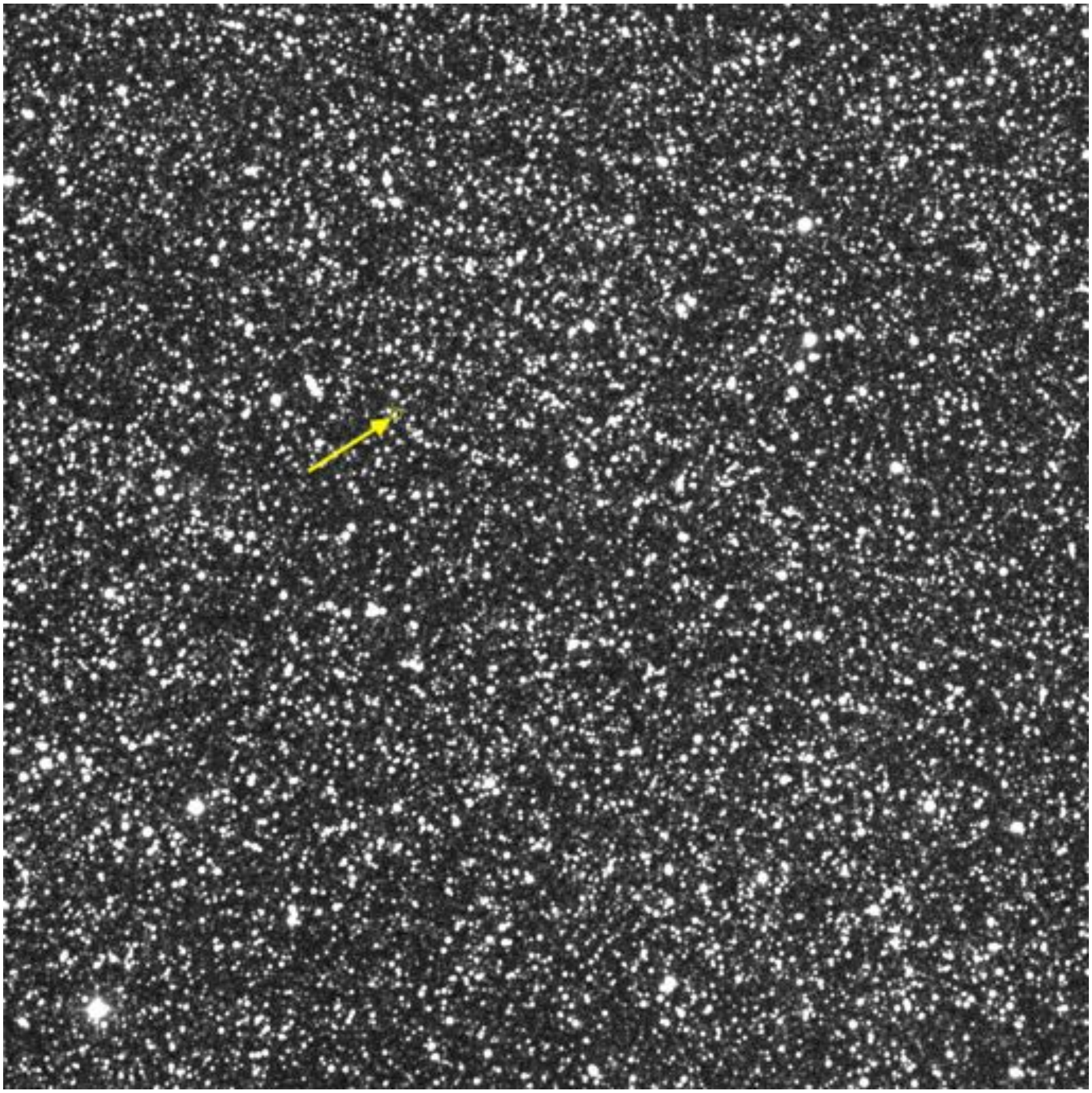

Figure 2.3: The master image used for the P1_AU dataset. The yellow arrow and circle show the position of V1835 Aql on the image.

Using two or more filters provides several advantages over using just a single filter. It allows determination if a star is changing its effective color with time, something that is critical for determining the characteristics of variable stars. Also, if the light curve behaves similarly in several filters it makes it much more likely that any observed variability is

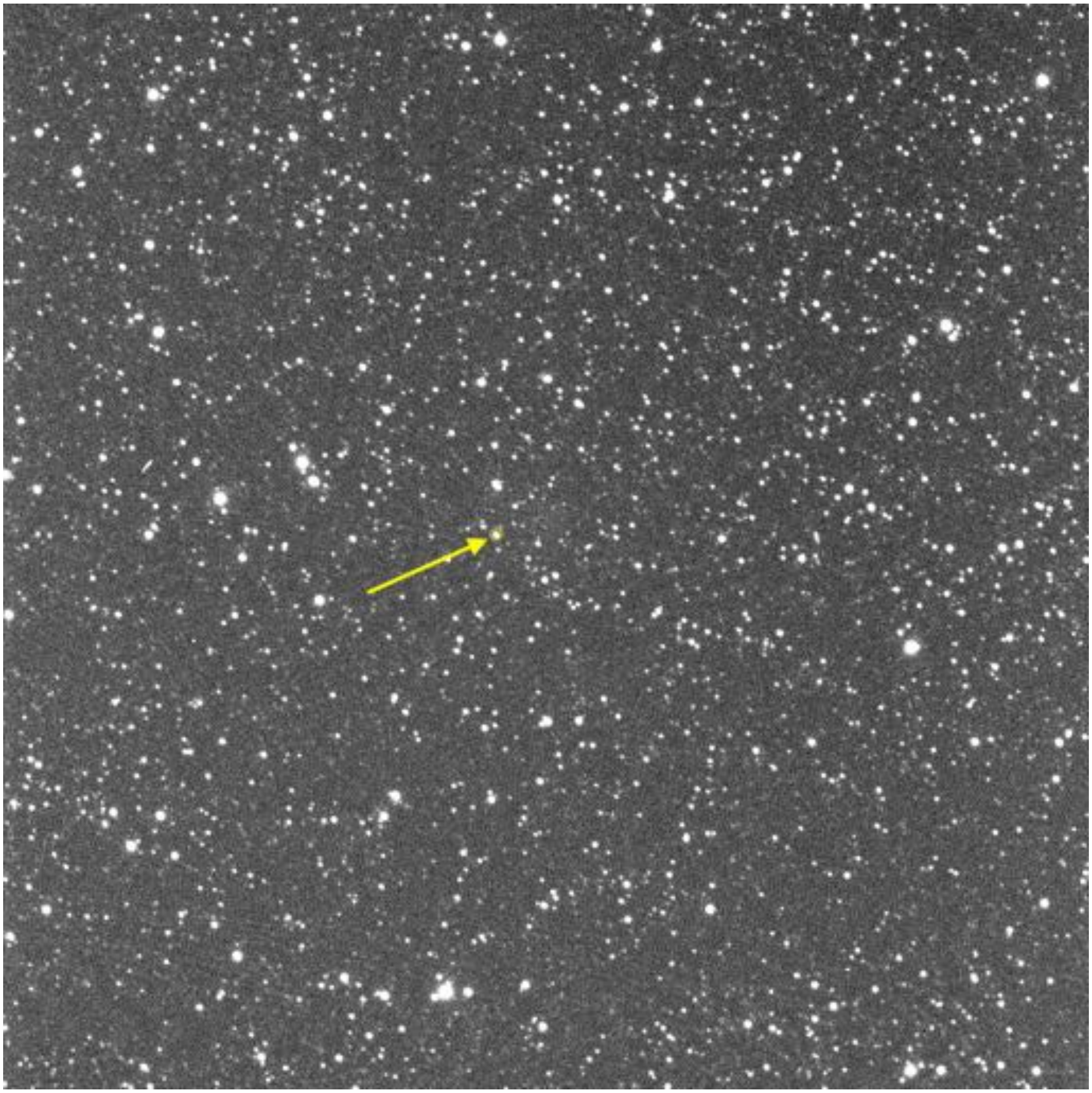

Figure 2.4: The master image used for the P5_AA dataset. The yellow arrow and circle show the position of V1835 Aql on the image.

real. Using two different colors also allows drawing a color-magnitude diagram (CMD) and examining where the variable stars land on the CMD which will help to determine at which stage of evolution a star may be.

2.3 Image Calibration

Once the raw images have been taken by the telescope they must be calibrated using bias, flat, and dark frames to remove imperfections introduced by the CCD. All of this is done automatically by the Skynet and Terminator systems that control the PROMPT telescopes. A bias frame is used to remove the low intensity bias signal that any CCD has. This charge is intentionally placed there to fill any traps that might exist on the CCD and it typically varies across the CCD. To determine the master bias frame, a series of 0-second exposure images are taken with the shutter and dome closed. These frames are then averaged and that average frame is subtracted from the raw images. A dark frame is similar to a bias frame except that it has a non-zero exposure time (40 s for PROMPT). While a CCD is exposing, a signal can be generated by random movements of thermally excited electrons. By scaling the dark frames to match the exposure time of a given image this dark signal can be subtracted away. A flat field is used to determine how sensitive different parts of the CCD are to light. Flat fields are taken by exposing the CCD to an object of uniform brightness; PROMPT uses the twilight sky. Since CCDs have different sensitivities in different filters flat fields need to be taken with each filter. Flats can also detect dust on the filters. By combining all of these calibration images the Skynet system automatically calibrates the original raw images effectively and quickly. Once the images are calibrated they are automatically made available to the individual who requested them via the Skynet website.

CHAPTER 3

PHOTOMETRY

To do our photometry we used a collection of software by Dr. Peter B. Stetson: DAOPHOT II, ALLSTAR, ALLFRAME, and DAOMASTER [16]. This suite of software can calculate the magnitude of every star in every image. These data can then be used to create a color-magnitude diagram (CMD), generate light curves for each star, and search for variable stars using statistical methods. To use this software each data set had to be split up by filter, e.g. P5_AU became P5_AU_I and P5_AU_V.

DAOPHOT operates by searching an image for areas that are brighter than a given threshold, then it fits a point spread function (PSF) to that bright area. The shape of this PSF can be allowed to vary across the image in a couple of different ways and the choice is referred to as the order of the PSF. The shape of the PSF can be varied linearly along x and/or y or quadratically across x and/or y. The reason for this is two fold, the focal plane of the telescope is a parabola but the CCD is flat and some telescopes have a slight astigmatism. DAOPHOT calculates a single PSF model for the image by searching the image for bright, uncrowded stars, iteratively subtracting any surrounding stars, and then averaging the resulting PSFs into a single PSF for the entire image. Typically this PSF was allowed to be a linear function of the x and y position on the images, though on images with a low number of PSF stars it was only allowed to vary in x or y, not both. DAOPHOT can determine whether or not an object is a star by examining its profile. As shown in Figure 3.1 the profile of different types of objects varies significantly so it is easy to determine if a given object is a star, a galaxy, or something else. This PSF fitting process is then repeated for each image in the data set.

Using the image's PSF, DAOPHOT searches through the image to find each star and determine its exact x, y position on the image. Then ALLSTAR takes these positions and scales the PSF to fit each star. The scaling factor used to scale the PSF for a given star is then used to determine the instrumental (not standard) magnitude of the star. This is done with Equation 3.1, where m is the instrumental magnitude, S is the scale factor, and C is a user selected constant, 25 in our case.

$$m = -2.5 \log_{10}(S) + C \tag{3.1}$$

This process results in a file with estimates of each star's position, magnitude, and the sky brightness. Despite initial difficulties, modulating settings within the programs (order of the PSF, threshold value, etc.) proved effective in producing results consistent with what appeared on the image. This was determined by searching plotting dots on the image where DAOPHOT found stars to make sure there were no false positives or false negatives. DAOPHOT and ALLSTAR typically found around 11,000 stars per image in the P1_AU dataset and around 3,000 in the P5_AU and P5_AA datasets, fewer due to P5's smaller field of view. Variations in the number of stars found image to image are due to changes in seeing, clouds, and background sky level (often due to moonlight). These variations can cause up to around 80% of the stars not to be found, though typical variations are $< 15\%$.

Once a list of each star on every image is generated DAOMASTER is used to create a coordinate mapping from one image to another. When ALLSTAR runs it assigns an ID number to each star, but since ALLSTAR processes a single image at a time the same star might have a different ID and position on each image. DAOMASTER takes a master image, selected manually to be of good quality and depth, then finds and uses a simple polynomial mapping function to convert the coordinate system of each subsequent image to the master so that a given star can easily be identified across all the images. Determining the polynomial fit is iterative and user guided but mostly automatic. Since the exact pointing of the telescope varies slightly from image to image DAOMASTER also adds stars that are off the edges of the master image to the master list of stars.

Several significant problems had to be overcome before accurate mappings could be

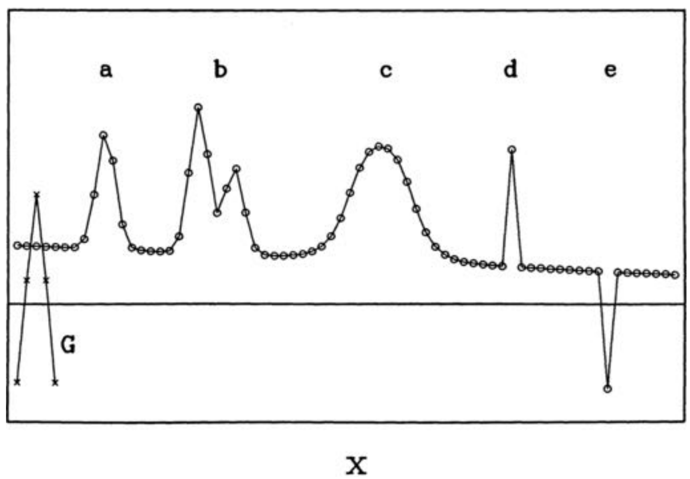

Figure 3.1: A 1-dimensional example of the profiles of different types of objects. The y-axis is counts on the CCD and the x-axis is position. (G) is the PSF generated by DAOPHOT, (a) is a star, (b) is two overlapping stars, (c) is a galaxy or nebula, (d) is a cosmic ray, and (e) is a low-valued bad pixel. This figure originally appeared in Stetson 1987, which can be found at https://doi.org/10.1086/131977[16]

generated by DAOMASTER. The causes of these problems were several significant rotations and scale changes in the images caused by the use of different telescopes, CCDs, and possibly due to the CCD being removed for maintenance. To resolve these issues, the P5_AU and P1_AU datasets had to be split into several smaller sets and processed separately with DAOMASTER. Then DAOMASTER was used to combine these smaller sets.

The final step is to search for very dim stars on each image. This is done by feeding ALLFRAME a list of the positions of all the stars on a very deep image. ALLFRAME then uses this list of known stars to look for stars that are very close to the noise floor in the shallower image. After this, DAOMASTER is run again to recombine the data from the images. DAOMASTER outputs several files of data, the two most relevant ones are the `.mag` and `.cor` files. The `.mag` file has the magnitude for each star averaged over the entire dataset while the `.cor` file has the magnitude for each star on each image. In the end this process located and determined magnitudes for roughly $11,600$ stars in the P1_AU images and roughly $3,000$ stars in the P5_AU and P1_AA data sets.

CHAPTER 4

CALIBRATION

DAOPHOT outputs instrumental magnitudes that are calculated from an arbitrary zero point so all the magnitudes are systematically offset from their standard values on the Johnson-Cousins photometric system. Calibrating these instrumental magnitudes to magnitudes on the standard scale requires using reference stars with known standard magnitudes. The instrumental and standard magnitudes of these stars can then be used to determine the systematic transformation that must be applied to all of the stars.

The reference stars used to calibrate the data in this study originally had their standard magnitudes in V, R, and I determined by Wehrung et al. (2013) and their standard B magnitudes were found in the AAVSO Photometric All-Sky Survey (APASS)[14, 17, 18]. The V, R, and I standard magnitudes for the reference stars had been found by taking images of standard stars[19] on three photometric nights; two nights at the BG telescope in V and I and one night with PROMPT C5 in V, R, and I. These images of standard stars were used to calibrate 15 secondary standard stars in the BGSU telescopes field of view, but only eight of these are within PROMPT C5's smaller field of view. No B images were obtained by Wehrung et al. (2013) so the standard magnitudes in B for these reference stars had to be found elsewhere. In this case APASS was used[17, 18]. The reference stars were found in APASS Data Release 9 by their right ascension and declination before their B magnitudes were used for calibration in the same way as the standard magnitudes from Wehrung et al. (2013). Due to the much larger error bars on the APASS data (often 0.1 to 0.3 mag) compared to the data from the PROMPT telescopes (0.01 to 0.05 mag), and the faintness of the PROMPT B images, the B data have significantly larger uncertainties when compared to the V, I, and R data.

Fitting a relationship between the standard and instrumental magnitudes in any two filters is required for the calibration of the instrumental magnitudes. This is because this technique allows consideration of the color of the star, not just its magnitude in a single filter. The calibration for the V and I data were done with V and I, the R data were calibrated using V and R, and the B data were calibrated using B and R. The calibration can be done with any pair of filters but only V and I will be shown in the following equations for simplicity.

Calibration was done in three major steps. The first major step uses the instrumental magnitudes of the reference stars in the `.mag` file and the standard magnitudes of the reference stars. The instrumental magnitudes in the `.mag` file are not the time-series instrumental magnitudes for each star on each image but are the instrumental magnitudes averaged over the entire dataset. The instrumental magnitudes of the reference stars were extracted from the `.mag` file and a least squares fit of $(v_{r,mag} - V_r)$ vs. $(V_r - I_r)$ and $(i_{r,mag} - I_r)$ vs. $(V_r - I_r)$ was performed where $v_{r,mag}$ and $i_{r,mag}$ are the instrumental magnitudes and V_r and I_r are the standard magnitudes. The second major step also uses the instrumental magnitudes in the `.mag` file, but in this step uses all of the stars, not just the reference stars. These instrumental magnitudes and the coefficients from the least squares fit, are used to determine an average standard V and I magnitudes for every single star in each dataset. The third major step uses the average standard color value found in the previous step along with the data from the time-series `.cor` file. The instrumental magnitudes in the time-series `.cor` file are the instrumental magnitudes for each star on each individual image. The image-by-image instrumental magnitudes can then be calibrated to the standard system using the standard magnitudes of the reference stars and the instrumental magnitude of the reference stars along with the least squares fit and $V - I$ color found in the previous steps.

The plots of $(v_{r,mag} - V_r)$ vs. $(V_r - I_r)$ and $(i_{r,mag} - I_r)$ vs. $(V_r - I_r)$ are of the form $y = \alpha + \beta x$. The zero point shift, α, depends on time dependent conditions like sky transparency, whereas the color coefficient, β, depends on time independent conditions such as the filter and CCD wavelength response. To avoid needing to calculate a new α for every image, differential photometry was performed (Step 3). Differential photometry eliminates explicit dependence on α in the calibration of the time-series magnitudes.

Step 1

The first major step (performing a least squares fit on $(v - V)$ vs. $(V - I)$ and $(i - I)$ vs. $(V - I)$ for the reference stars) was done using the RAF command `curfit`. This was done to find the zeroth and first order coefficients (α and β) in Equations 4.1 and 4.2.

$$v_{r,mag} - V_r = \alpha_v + \beta_v(V_r - I_r) \tag{4.1}$$

and

$$i_{r,mag} - I_r = \alpha_i + \beta_i(V_r - I_r) \tag{4.2}$$

where $v_{r,mag}$ and $i_{r,mag}$ are the averaged instrumental magnitudes from the `.mag` file, the r subscript indicates reference stars, and V_r and I_r are the standard magnitudes of the reference stars.

Step 2

The second major step (finding an average color for every star in the dataset) was done by subtracting Equations 4.1 and 4.2 and rearranging them to get the system of equations in Equation 4.3

$$\begin{pmatrix} (1+\beta_v) & -\beta_v \\ \beta_i & (1-\beta_i) \end{pmatrix} \begin{pmatrix} V_{f,mag} \\ I_{f,mag} \end{pmatrix} = \begin{pmatrix} v_{f,mag} - \alpha_v \\ i_{f,mag} - \alpha_i \end{pmatrix}, \tag{4.3}$$

where $v_{f,mag}$ and $i_{f,mag}$ are the averaged instrumental magnitudes from the `.mag` file, the f subscript indicates non-reference, or field, stars, and $V_{f,mag}$ and $I_{f,mag}$ are the averaged standard magnitudes. Subtracting these two magnitudes give the $V - I$ color index needed for the third major step

Step 3

The third major step (calibrating the instrumental magnitudes for each star on each image) was done using the time-series instrumental magnitudes in the `.cor` file. This can be done by using the α and β values found in the first step in slightly modified versions of Equations 4.1 and 4.2 that have been altered to use the values from the `.cor` file instead of the values from the `.mag` files.

$$v_{r,cor} - V_r = \alpha'_v + \beta_v(V_r - I_r) \tag{4.4}$$

$$i_{r,cor} - I_r = \alpha'_i + \beta_i(V_r - I_r) \tag{4.5}$$

$$v_{f,cor} - V_f = \alpha'_v + \beta_v(V_{f,mag} - I_{f,mag}) \tag{4.6}$$

$$i_{f,cor} - I_f = \alpha'_i + \beta_i(V_{f,mag} - I_{f,mag}) \tag{4.7}$$

where the *cor* subscript indicates time-series values from the `.cor` file, the r subscript indicates values from the reference stars, and the f subscript indicates values from the non-reference stars. All of the primed α values will subtract away when solving for the time-series magnitudes V_f and I_f. Solving this system of equations for the standard, time-series magnitudes V_f and I_f yields Equations 4.8 and 4.9

$$V_f = v_{f,cor} - v_{r,cor} + V_r - \beta_v((V_{f,mag} - I_{f,mag}) - (V_r - I_r)) \tag{4.8}$$

$$I_f = i_{f,cor} - i_{r,cor} + I_r - \beta_i((V_{f,mag} - I_{f,mag}) - (V_r - I_r)). \tag{4.9}$$

There is one value of V_f and I_f for each reference star so these values of V_f and I_f are averaged together to find the standard magnitude for that non-reference star on a particular image. Note that alpha, which depends on time-variable conditions like sky transparency, has disappeared. β should be reasonably consistent over time because it is due to constant condition such as the filter and CCD wavelength response. Differential photometry (Equations 4.8 and 4.9) is done so that the time dependent α term does not explicitly affect the calibration on each image.

Implementation

An original Python program was written to implement the conversion from the instrumental magnitudes to standard magnitudes (see the appendix for the code). To check that the program performed the calibration correctly, the calculated standard magnitudes of the reference stars from Equations 4.3, 4.8, and 4.9 were checked against the known standard magnitudes from Wehrung et al. (2013) and APASS. While there was some deviation from the known standard magnitudes for the reference stars, the standard deviation of the differences was only 0.01 mag, similar to the photometric uncertainties given by DAOPHOT. The standard magnitudes were also searched for any anomalously high or low values and none were found. Additionally, a color-magnitude diagram and several light curves of the comparison stars were generated in order to look for systematic issues in the calibration and none were found. The results of these tests show that the program performs correctly.

CHAPTER 5

COLOR-MAGNITUDE DIAGRAM (CMD)

The importance of plotting a color-magnitude diagram (CMD) cannot be overstated. Not only does the shape of the CMD provide an excellent confirmation that the photometric calibration is accurate, it also provides information that can be used to classify variable stars. For instance, if a previously classified LPV does not appear on the red giant branch (RGB), it was probably misidentified as a LPV. The P1_AU data set was used to generate the CMD (Figure 5.1) because the PROMPT C1 telescope has a much larger field of view than the telescope used for the other data sets (PROMPT C5) and therefore has more stars: $11,600$ vs. $3,000$. Most CMDs presented in the literature are of star clusters, so they have distinct sequences. These distinct sequences are caused by several things: the cluster stars are all at the same distance so the apparent magnitude is an analogue for the absolute magnitude, cluster stars are all the same age and so they will have a well-defined sequence, including the main-sequence turn off, and all the cluster stars are the same metallicity, which yields tight sequences since the metallicity of a star can significantly affect its spectrum. Our data are of field stars so the sequences will be broad and overlapping since the stars are all of different distances, ages, and metallicities.

From Wehrung et al. (2013) we know that the reddening for V1835 Aql is about $E(B-V) = 0.67$ mag, though there is considerable uncertainty about the exact value. However, the CMD is plotted as V vs. $V-I$, so $E(V-I)$ must be calculated. To do this, the formula $E(V-I) = 1.24 \times E(B-V)$ provided by Layden et al. (2003) is used to find the horizontal component of the reddening vector, giving $E(V-I) = 0.83$ mag. The vertical component of the reddening vector is given by $A_V = 3.1 \times E(B-V)$, where A_v is the interstellar absorption, and was found to be $A_v = 2.08$ mag[20].

Since the stars in the field are all at different distances this reddening can only be applied to V1835 Aql with any confidence. V1835 Aql is at the location $(l, b) = (34^\circ.8313, -3^\circ.5974)$

which puts it in, or nearly in, the disk of the galaxy. At this galactic latitude the reddening could vary significantly across the field of view. However, when de-reddening several of the variable stars then determining their spectral type from their color it is found that their position on the CMD is approximately what would expected of a star of that spectral type. As a result,V1835 Aql's de-reddening values have been applied to determine the approximate spectral types of some of the variables.

Long Period Variables are cool giants or supergiants burning elements heavier than hydrogen in their core we would expect most of the LPVs that were detected to lie off the main sequence. As expected, most of the LPVs are very clearly post-main sequence stars, as shown in Figure 5.1, including V1835 Aql, which is found squarely in the middle of the red giant region.

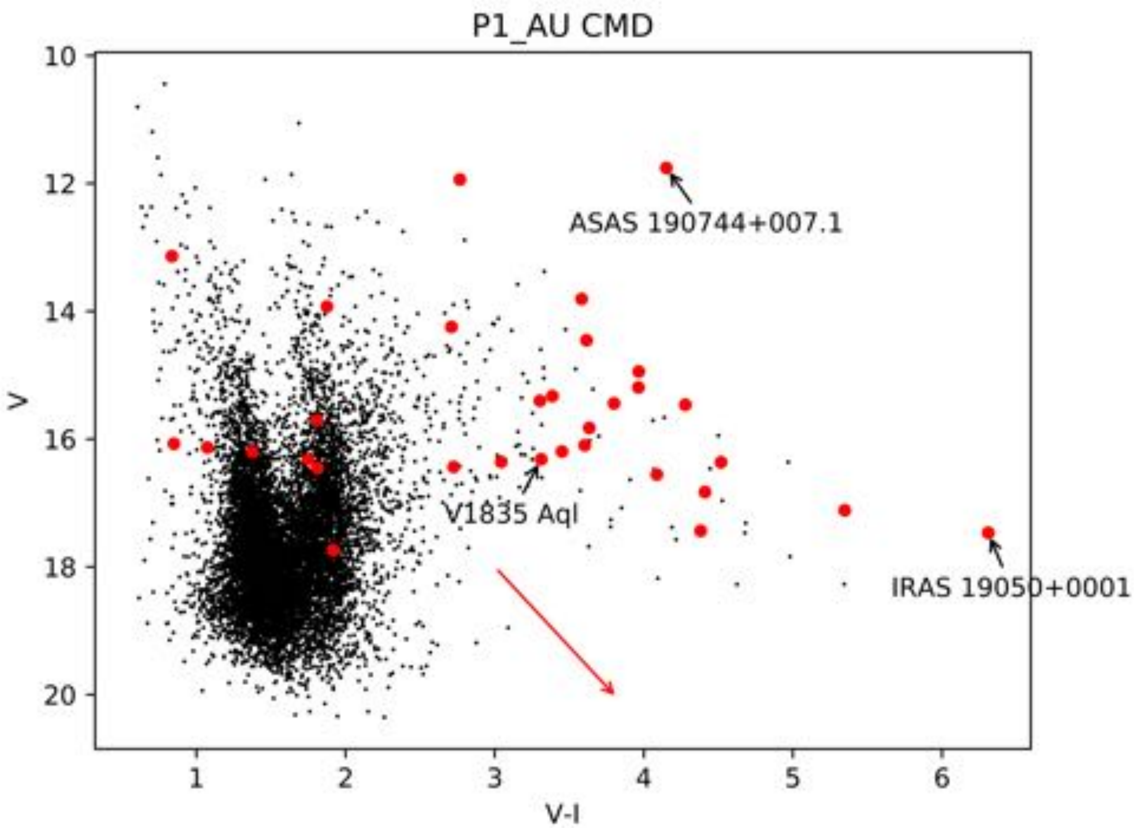

Figure 5.1: CMD of the P1_AU field. Variable stars are highlighted in red. V1835 Aql and a two other notable variables are also labeled. A reddening vector for V1835 Aql is shown at the bottom. The main sequence is the leftmost branch and the right branch is made of stars that have aged off the main sequence. The low density scatter of stars with $V - I$ values > 2.5 or so are in the red giant branch. While there are many more specific sequences visible in an ideal CMD they are not distinct in this CMD due to the broadening of each sequence as a result of not being able to control for metallicity, distance, and age.

CHAPTER 6

V1835 AQL

V1835 Aql has been studied many times in the last 15 years. Previous studies have all relied on glass plates in the Harvard collection, a single spectrum, or time-series photometry with a very short time base; this is the first study with a time base suitable V1835 Aql's several hundred day period. While the Harvard plates provide a rough light curve (LC) of V1835 Aql during its outburst in 1899 through 1911, the information they provide is severely limited. There are only 175 plates to document the 100 year period between 1888 and 1988. Even these data are limited because they only cover a single band (blue) and in most observations post-outburst V1835 Aql lies below the detection threshold, which was typically a photo blue magnitude of $m_{ptg} = 15$ mag[1]. The two spectra taken, which only cover the visible through mid-infrared, are sufficient to identify V1835 Aql as a symbiotic star (SySt), but do not shed any light on whether or not the color changes throughout its orbit and provide only minimal insight to the geometry and interaction within the system.

The data from this study do provide that information, the light curve of the data can be seen in Figure 6.1. This LC was generated by omitting those data points whose uncertainty is more than three standard deviations above the average uncertainty and then averaging all the images for a given night into a single point. As shown in Figure 6.1, the B and R data have much smaller time coverage than the V and I data. The reason that, especially in B and V, the error bars get rapidly larger near the minima is that the star is getting dim enough to approach the detection threshold. Near this the uncertainty grows rapidly. The uncertainty for the error bars is provided by DAOPHOT.

A summary of the results of this study of V1835 Aql can be found in Table 6.1. The angle brackets indicate time-averaged data.

Table 6.1: V1836 Aql Results

Orbital Period	RA	Dec	$\langle B \rangle$	B_{min}	B_{max}	$\langle V \rangle$	V_{min}	V_{max}
419 ± 4 days	19:07:42.40	0:02:51.0	17.85	18.58	17.34	16.03	16.72	15.43

$\langle R \rangle$	R_{min}	R_{max}	$\langle I \rangle$	I_{min}	I_{max}	$\langle V-I \rangle$	$(V-I)_{min}$	$(V-I)_{max}$
14.41	14.98	14.05	12.85	13.14	12.70	3.18	3.75	2.68

6.1 Period Analysis

There is clear periodic behavior in the LC for V1835 Aql so a Fourier transformation was performed on the V and I time series data using the Date Compensated Discrete Fourier Transform (DC DFT) algorithm in the VSTAR program provided by the American Association of Variable Star Observers (AAVSO). After performing the DC DFT, VSTAR shows a spectrum of all the periods from 10 to 1000 days, at a step size of 0.1 days, plotted against their power, the amplitude of that period. The power vs. period graph for V1835 Aql in the I band is shown in Figure 6.2. The B and R data were not used due to the larger uncertainties in the B data (0.1 mag instead of 0.01 mag) and the much shorter time base as shown in Figure 6.1. VSTAR found a very strong single period at 416 ± 12 days in I and 422 ± 13 days in V; averaging these two periods gives a period of 419 ± 12 days. Experience has shown that the periods found by VSTAR with the data from this study are accurate to around 3% which is how the uncertainty in the period was determined.

To provide a clearer picture of the dynamics in V1835 Aql a phased LC was made. A phased LC is generated by determining the phase of each data point then graphing magnitude vs. phase instead of magnitude vs. time. This is done by transforming the time domain into the phase domain through Equation 6.1:

$$\phi = \frac{t - t_{min}}{P} - \lfloor \frac{t - t_{min}}{P} \rfloor \tag{6.1}$$

where ϕ is the phase, t is the Heliocentric Julian Date (HJD), t_{min} is the minimum HJD, P is the period in days and $\lfloor x \rfloor$ indicates the integer portion of x. Phased LCs are useful since by transforming from the time domain to the phase domain the effective sample rate is significantly increased. This often reveals small, hard to see features in the LC. Figures 6.3-6.5 are the phased LCs for V1835 Aql and are simply the same data graphed in different ways to make different features of the LCs clearer. In these figures, especially Figure 6.4, there are quite clearly two different minima. The larger, primary minimum is at a phase of about 0.70 and has an amplitude of 0.2 mag to over 1 mag, depending on the filter. The smaller, secondary minimum is at a phase of about 0.15 and has an amplitude of just under 0.1 mag in V and I. It is not sampled well enough in B and R to get a clear idea of its amplitude. While there are some gaps in the B and R phased LCs, Figure 6.3 shows that in spite of this the extrema of the LC are reasonably well sampled in both B and R and so the B and R extrema values in Table 6.1 are probably accurate.

6.2 Source of Variability

A SySt is a close binary system with a cool, diffuse component and a hot compact component. The variability in a SySt could come from a variety of different sources or combination of sources. The simplest possibility is that of purely ellipsoidal variability. In the generalized case, ellipsoidal variability is caused by tidal distortion of one or both of the stars in a binary system. In most close binaries, like a SySt, it would be expected that the orbits of the stars are circular since non-circular orbits would introduce significant gravitational drag, that would quickly circularize the orbits. By the same mechanism it would be expected that the red giant is tidally locked.

In these binary systems the area where a test mass is gravitationally bound to a particular star is not radially symmetric around each star. Instead, it is slightly teardrop shaped with the point of the teardrop pointing towards the other star. This teardrop shape is called a Roche Lobe and is defined by the surface of the equipotential whose potential is equal to the potential of the L1 Lagrange Point, which is at the tip of the teardrop. In a reference frame that rotates with the system this effective potential is a combination of gravitational potential and angular momentum and is called the Roche Potential. As a star evolves and expands, its size can become significant when compared to its Roche Lobe. When this happens the star will start to be distorted by the Roche Potential and begin to assume the same teardrop shape as the Roche Potential. This distortion is called tidal distortion. If the star gets so large that it fills its entire Roche Lobe then either the star will start to lose mass to its companion star or the outer layers of the star will become unbound from the star and begin to orbit the system as a whole.

As a tidally distorted star rotates it would be expected that the binary would have two minima per orbital period, one for each time that the point of the Roche Lobe (L1) is pointing towards or away from an external observer and the star appears round. These minima would be similar to each other in amplitude across all filters, with variations not more than around 0.2 mag in I [21], and the $V - I$ graph would be nearly a flat line. The reason that the color does not change is because, while the star's apparent size is changing significantly, it is still monochromatic, which is to say that the effective temperature of its photosphere does not change significantly with respect to position on the star. V1835 Aql does show two minima per orbital period, when phased at 419 days (Figure 6.4), but they differ in amplitude significantly, far more than would be expected from a purely ellipsoidal variability. The secondary minimum has an amplitude of about 0.1 mag in I and creates a flattening in V, which is consistent with an ellipsoidal variable. However, the primary minimum's amplitude is 0.44 mag in I and 1.29 mag in V, far to large to be due solely to ellipsoidal variability. This large discrepancy between the amplitudes of the two minima also results in a large change in color $(V - I)$ throughout the orbit which is not consistent with ellipsoidal variability. These inconsistencies with a monochromatic ellipsoidal model show that while it is possible that the secondary minima is due to ellipsoidal variability it does not explain the larger scale variability of V1835 Aql.

The next simplest scenario is that the red giant is tidally distorted and monochromatic but the compact star is hot enough to be visible despite its small size. If this were the case it would be expected that the large variations in color and magnitude are due to an eclipsing of the compact star by the red giant. This would lead to LCs that had low-level, ellipsoidal variability along with a very sharp-edged eclipsing event where the red giant eclipses the compact star and the system suddenly becomes dimmer and redder, remains at a constant brightness and color for brief time, then quickly returns to its pre-eclipse brightness and color as shown in Figure 6.6. The large color change is caused by the extremely blue light from the hot compact star being entirely blocked by the red giant, leaving only the light from the red giant visible. What is seen in fact is very different. V1835 Aql does become redder but there is no interval of constant color near the minimum (Figure 6.5) and the larger dimming event occurs from a phase of around 0.3 to 1.0. An eclipse cannot possibly occur for more than half the orbital period.

The next scenario is that the compact star is not visible but the red giant is tidally distorted and polychromatic. In this case, polychromatism is caused by the side of the red giant nearest the compact star being heated by radiation from the compact star. This so called "reflection effect" is a well known property of some close binary systems[22]. While the compact star is not very luminous, due to its small size, the red giant is large and very close and will therefore absorb a significant percentage of the light emitted from the compact star. If this were the case it would be expected that the LCs would be a superposition of two different LCs. One from the ellipsoidal variability which would have two small minima per period with amplitudes of less than 0.2 mag and the second would be a single, deep minimum as the heated part of the red giant rotated away from the observer, during which the system would become significantly redder. Adding together these two light curves would give the kind of LC that V1835 Aql has. V1835 Aql's LC has a single, deep minimum as the heated part of the red giant rotated away from the observer, during which the system became significantly redder. This is followed by a small minimum due to the ellipsoidal variability where there is no change in color.

It is possible to have both a polychromatic, tidally distorted red giant and a visible compact star contributing to the LC. However, in that situation it would be expected that the compact star would show up in the spectra and there is no evidence of a hot star in either of the visible spectra (4000-7000 Å) presented in Wehrung et al. (2013) and Bond & Kasliwal (2012) [14, 2].

With this analysis in mind it seems clear that V1835 Aql consists of a tidally distorted red giant star and a compact star, probably a white dwarf, that is heating one side of the red giant. Since emission from the system appears to be dominated by the red giant it is possible to determine approximate temperatures of each side of the red giant from the $V - I$ color. Using the polynomial fit given in Amado & Byrne (1996)[23], the differential temperature between the two sides of the red giant was found to be roughly 400 ± 34 K[23]. This temperature change seems consistent with the hypothesis of a closely orbiting, low luminosity white dwarf heating a red giant. V1835 Aql is consistent with an S-type symbiotic star due to the strong Hα lines and lack of mid infrared lines in its optical spectra[14, 2]. S-type SySts also have orbital periods on the order of a few hundred to a few thousand days and no Mira/LPV component, V1835 Aql is consistent with this as well.

Using 419 days as the orbital period the orbital separation can be easily calculated from Kepler's Laws.

$$(m_1 + m_2) = \frac{a^3}{P^2} \tag{6.2}$$

where m is in solar masses, a is in AU, and P is in years.

Mikolajewska (2003) provided masses of the giant and hot components for many SySts[24]. In these SySts the giant component's mass ranged from from 0.5-4.5 $M_{\odot}$ and the hot component's mass ranged from 0.31 to 1.4 $M_{\odot}$[24]. Using the minimum and maximum values for the system mass gives bounds on the orbital separation which are 1.0 to 1.9 AU. Performing an error weighted average on the masses given in Mikolajewska (2003) gives an average mass for the giant component of 1.2 $M_{\odot}$ and a mass of the hot component of 0.47 $M_{\odot}$. Putting these values into Equation 6.2 gives an orbital separation of 1.6 AU for V1835 Aql.

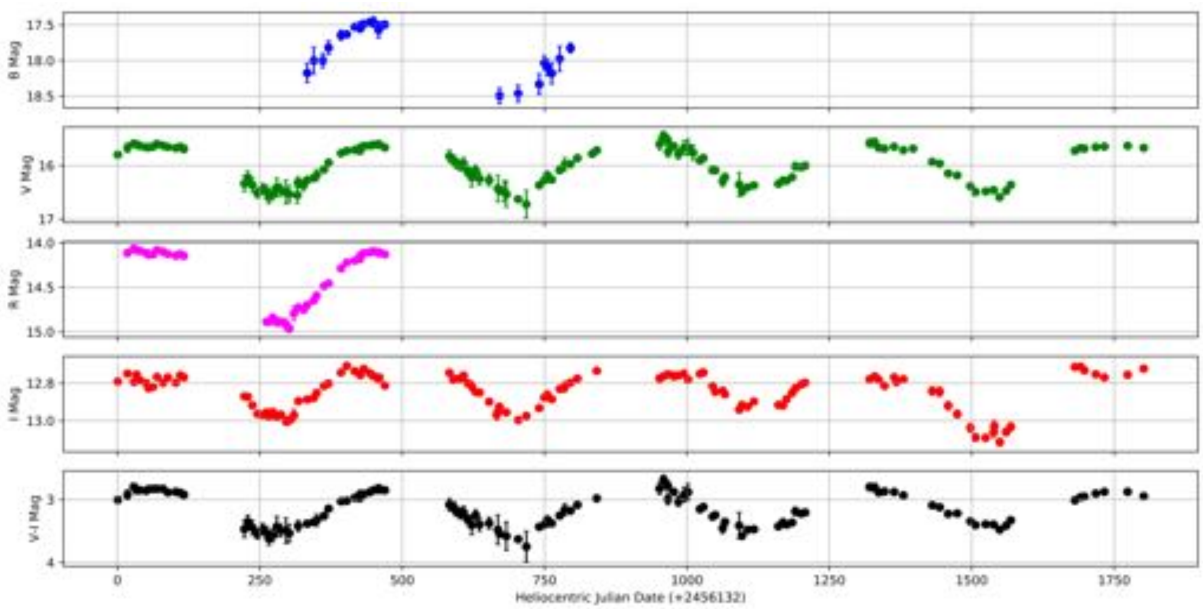

Figure 6.1: The LC of V1835 Aql. All figures in this chapter will adhere to the following color scheme: B data will always be shown in blue, V data in green, R data in magenta, I data in red, and $V-I$ data in black. Note the large changes in color $(V-I)$ with time. The uncertainty for the error bars is provided by DAOPHOT.

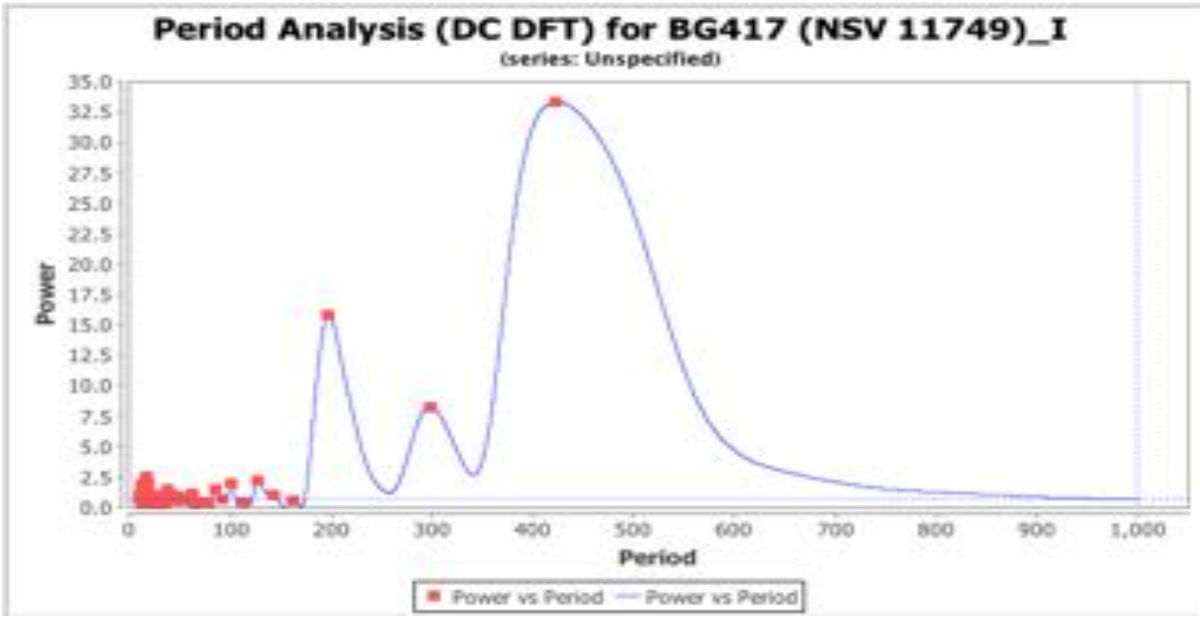

Figure 6.2: Power vs. period for V1835 Aql. The 419 day period is clear. The 200 day period is an alias of the 419 day period

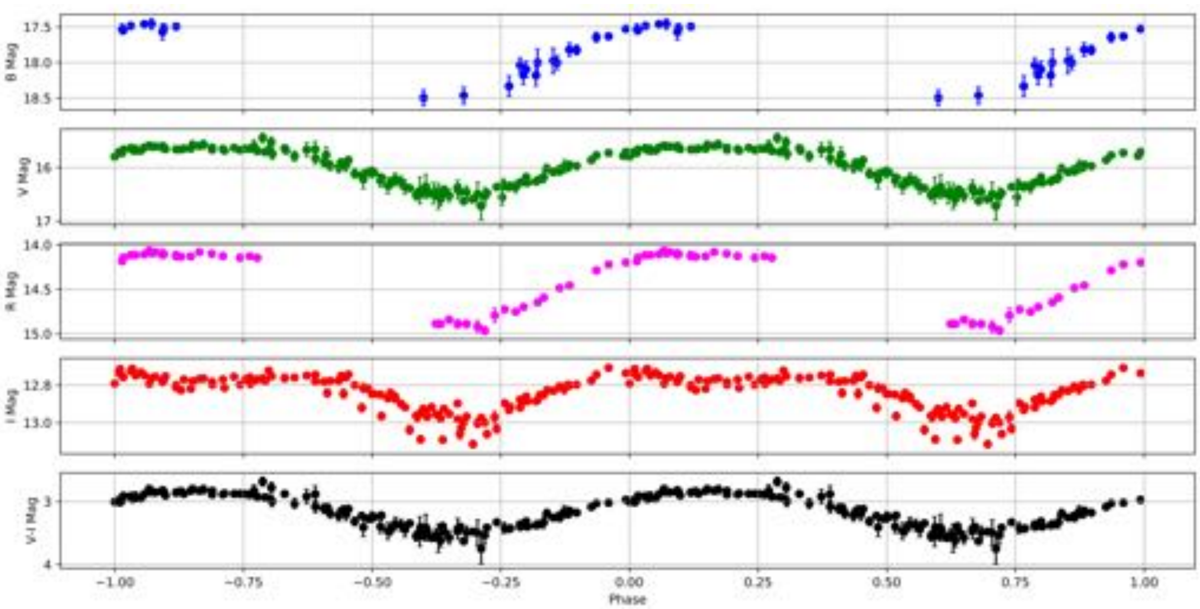

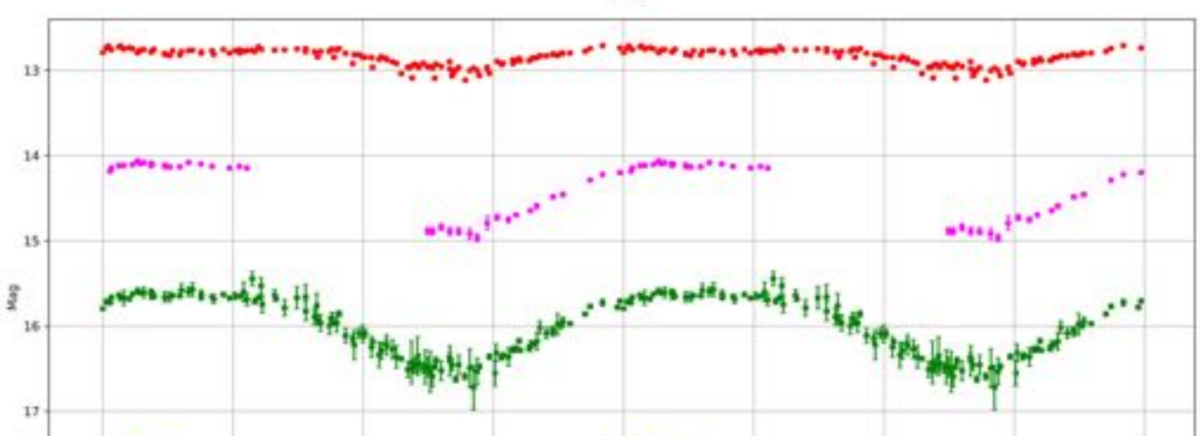

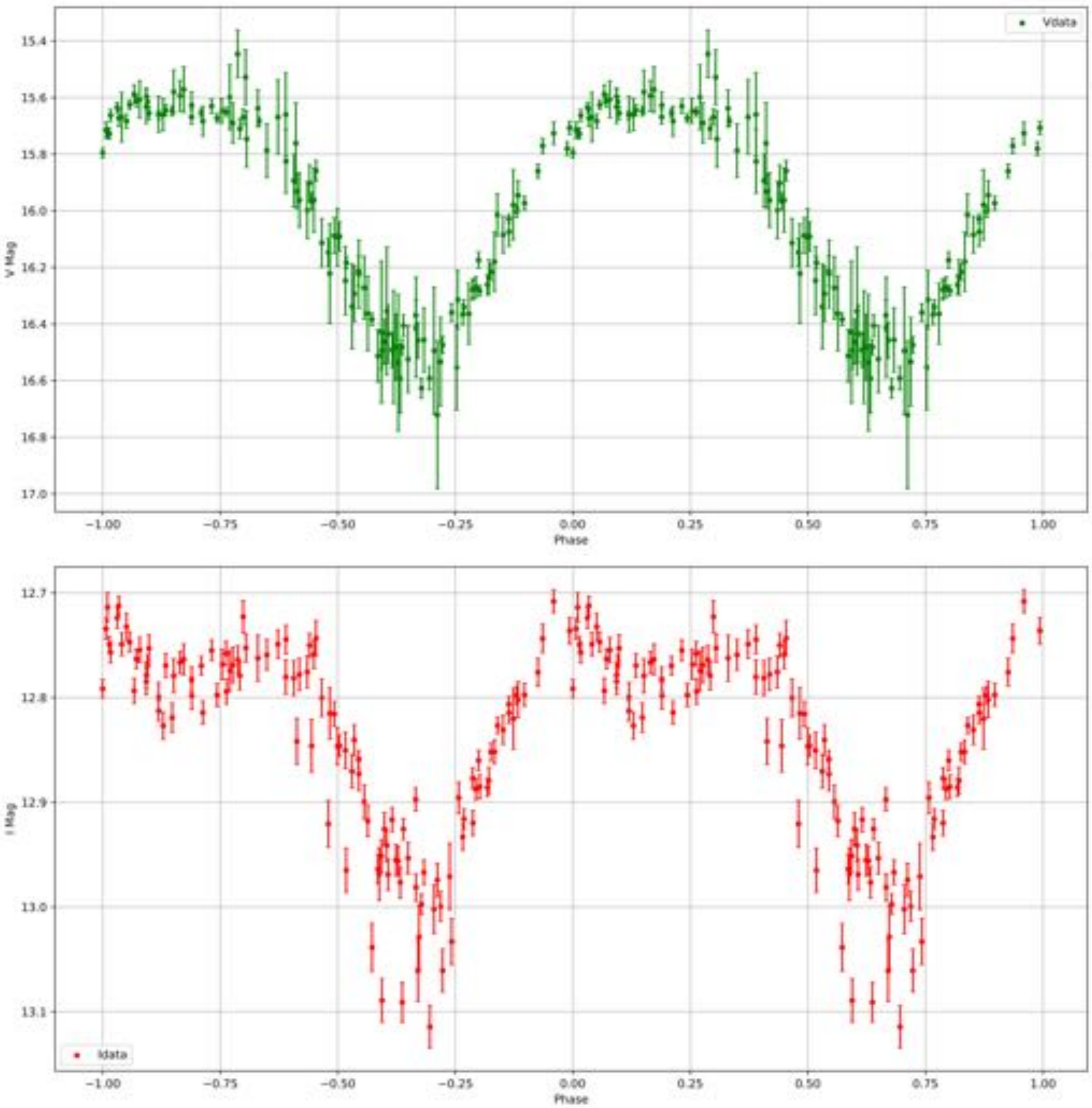

Figure 6.4: 419 day phased LCs of V1835 Aql. **Top** is the V data in green and **bottom** is the I data in red. The point colors are defined in Figure 6.1. Note the clear secondary minimum in I. The secondary minimum is visible in V, though due to the scale of the plots it is harder to clearly distinguish.

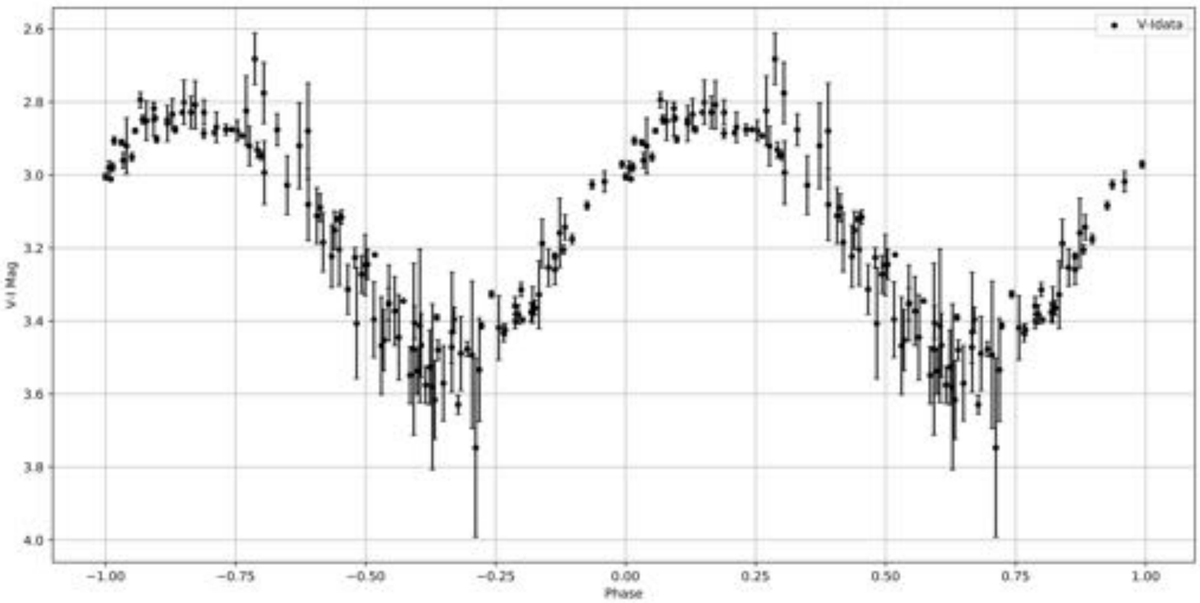

Figure 6.5: Phased LC of the $V - I$ data. Note the large change in color.

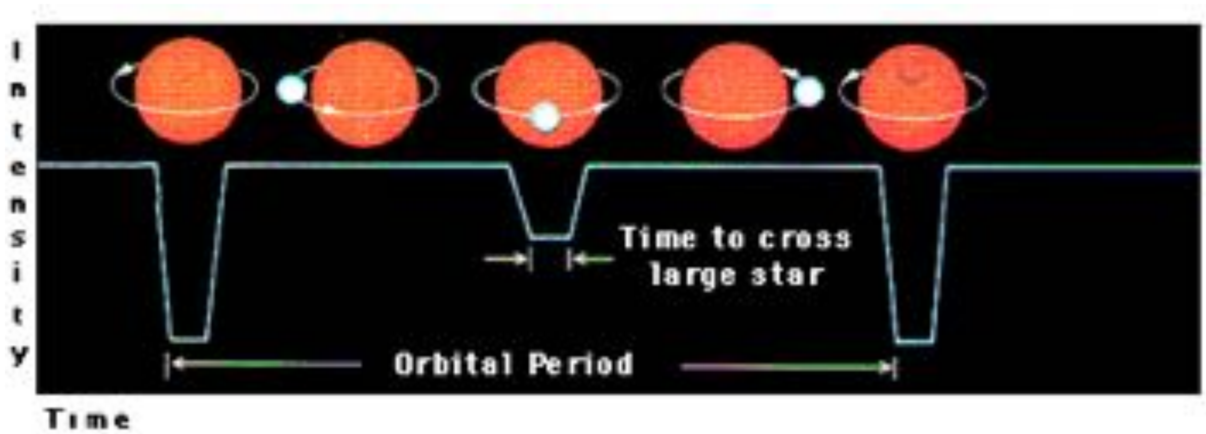

Figure 6.6: The extremely sharp decreases and increases in brightness indicative of an eclipsing binary are modeled in this synthetic plot from NASA. Note the section of constant brightness in each minimum. Retrieved from `https://imagine.gsfc.nasa.gov/educators/hera_college/binary-model.html` on April 19th, 2018.

6.3 Computational Modeling with PHOEBE 2.0

With the data provided by the light curves it is possible in principle to construct a 3-dimensional model of the binary system. The most widely used code that has been used for this is the Wilson-Devinney (WD) program[25]. However, this code was originally written in 1971 and even the more modern wrappers for it will often not run on current operating systems. The WD code also suffers from a lack of precision, due to computational constraints in the 1970s and missing physics, such as radiative and dynamical effects. While new physics has been incorporated into the WD code since its original development, it ultimately has not kept up with advances in the precision of photometric and spectroscopic measurements[26].

PHOEBE (PHysics Of Eclipsing BinariEs) was originally released in 2005 as a wrapper for the WD code. However, the developers of the first version of this program recognized the need for more advanced modeling software. Version 2.0 of PHOEBE was rewritten from scratch to address this need. PHOEBE 2.0 was chosen to make a model of V1835 Aql. Unfortunately, at this point in time PHOEBE 2.0 is still under heavy development and as a result not all features are available. While we have written a program that uses PHOEBE 2.0 to simulate an M3/M4 giant (the spectral type of the red giant in V1835 Aql[2]) and a white dwarf, and we can set all the appropriate parameters for the system, PHOEBE 2.0 does not currently support fitting a model to the given data. Once PHOEBE 2.0 is a more fully featured program a simulation of this system could be highly informative.

CHAPTER 7

OTHER VARIABLES

While the primary focus of this study was the SySt V1835 Aql, there was also a search undertaken for additional variable stars within the field of view. A total of 31 other variables were found, of which only 10 were already known. Detailed discussions of the light curves of five of these 31 variable stars are presented here. The other results are presented in Table 7.1, with brief comments on interesting features of specific variables in Section 7.3.6.

7.1 Search for New Variables

Generating LCs for each of the 11,000 stars in the data set and then visually examining them to determine variability would take far too long to be practical. Instead, the algorithm suggested in Welch & Stetson (1993) was used [27]. This algorithm requires the magnitude of a star in two different filters, V and I for this application, and returns a single number, called a variability index, which indicates whether or not a star is variable.

The first step in the algorithm is to determine the weighted mean magnitudes in each of two different filters:

$$\overline{V} = \frac{\sum_{j=1}^{n} \frac{V_j}{\sigma_{V,j}^2}}{\sum_{j=1}^{n} \frac{1}{\sigma_{V,j}^2}} \tag{7.1}$$

$$\overline{I} = \frac{\sum_{j=1}^{n} \frac{I_j}{\sigma_{I,j}^2}}{\sum_{j=1}^{n} \frac{1}{\sigma_{I,j}^2}} \tag{7.2}$$

where j indicates a given observation, n is the total number of observations, and σ is the uncertainty. The next step is to compute the magnitude residuals, δV_i and δI_i, when normalized with respect to magnitude:

$$\delta V_j = \frac{V_j - \overline{V}}{\sigma_{V,j}} \tag{7.3}$$

$$\delta I_j = \frac{I_j - \overline{I}}{\sigma_{I,j}}. \tag{7.4}$$

The variability index (I_{vari}) is then defined as

$$I_{vari} = \sqrt{\frac{n}{n-1}}\frac{1}{n}\sum_{j=1}^{n}(\delta V_j \delta I_j) = \sqrt{\frac{1}{n(n-1)}}\sum_{j=1}^{n}(\delta V_j \delta I_j) \tag{7.5}$$

where the factor of $\sqrt{1/n(n-1)}$ normalizes with respect to the number of observations. For random photometric errors δV_j and δI_j should be uncorrelated so their products should average to zero for a large number of observations. If there is a positive or negative correlation between δV_j and δI_j, then a significant variability index will occur.

The variability index vs. the V and I average magnitudes were plotted to get an idea of the distribution of the variability index (Figure 7.1). To make a final determination of whether or not a given star was variable the LCs of every star with a variability index > 1 were plotted and visually examined. Only two variable stars with variability index of < 2 were found so it is unlikely that any variable stars were missed in this search.

Stars with a large variability index that were determined to be non-variable were rejected for a few reasons. In many cases a single night would be far from average, giving an unusually large large I_{vari}, this is probably due to a cosmic ray or something similar interfering with the CCD. In the other cases there would be two non-variable stars very close to each other, close enough that on nights with poor seeing DAOPHOT treated them as if they were a single star so their light curves jump between the magnitudes of each individual star and the magnitude of the combined optical binary. This leads to an average value that is different from the magnitude of the individual stars or the combined stars so every single point has a large residual as calculate by Equations 7.3 and 7.4.

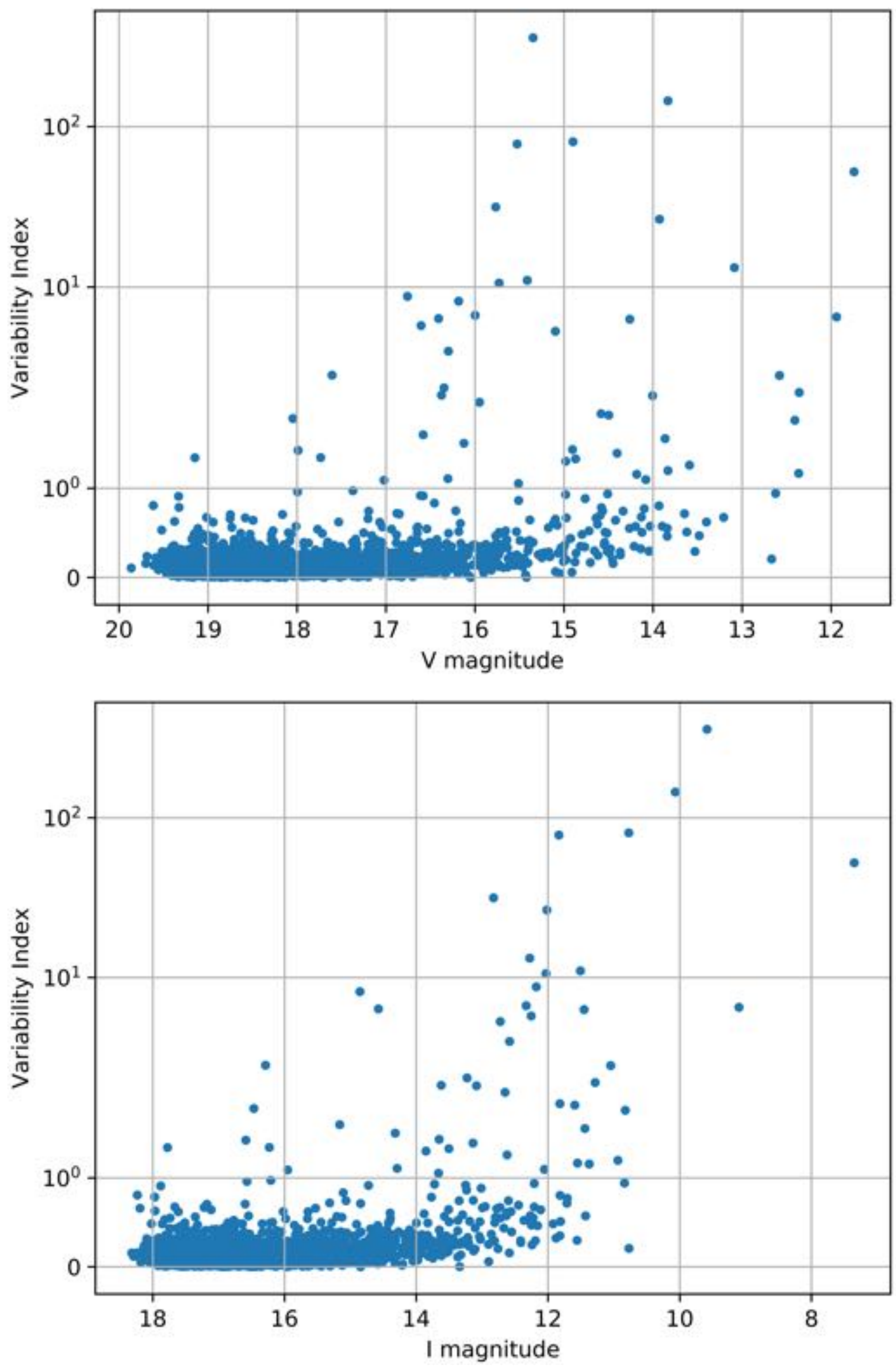

Figure 7.1: The variability index vs. the average V and I magnitude of a star.

7.2 Period Analysis

Similar to the period analysis done on V1835 Aql (Section 6.1), VSTAR's DC DFT algorithm was run on the V and I time series data of each variable star searching for periods between 10 and 1,000 days. These limits were chosen due to the time baseline and cadence of the observations. In total the data cover about 1,800 days with individual observations around 14 days apart. To accurately determine a period one needs to sample it well both during each period and for multiple periods. Periods longer than 1,000 days will only be sampled during one to two periods, which is insufficient to accurately determine a period. Periods that are very short, less than about a month, will only be sampled once or twice per period. This can be somewhat offset by how many periods are sampled but ultimately if the period is significantly shorter than the time between observations it is difficult to accurately determine a period. This is why the lower limit of 10 days was chosen.

In most variable stars found there was a single, predominant period. However, in several cases there is a clear secondary period. The dominant period is often easy to see by eye, however, some variables appear random until a DFT is performed on the data. The period(s) are reported in the "Period" column of Table 7.1. In data sets like this, periods can have aliases. These are periods found by the DFT that are not caused by actual periodicity in the star but by how the true periodicity interacts with the gaps between observations and the gaps between seasons. Using an excel widget written by Professor Layden that finds aliases for a given period, the periods returned by the DFT were examined and any aliases were identified and ignored. Determining the uncertainty for the periods was done by generating phased LCs for periods farther and farther from the period found by VSTAR until the phased LC no longer looked coherent. This point was found to be about 3% away from the period found by VSTAR.

7.3 Variable Stars

The Subsections 7.3.1-7.3.5 contain detailed discussion and figures of five of the most interesting variable stars in the dataset. These stars were chosen because they are uncommon types of variables or because they are typical for their variable type. Subsection 7.3.6 provides brief summaries and comments on any noteworthy features of particular variables. Table 7.1 provides information on all the variable stars in the field of view in tabular form. SKYNET includes coordinate transformations in their images so all right ascensions (RA) and declinations (Dec) were found by selecting the star in the program SAOImage DS9, a program for reading `.fits` files, and reading off the RA and Dec. The photometric values plotted in the figures were found by rejecting any data points whose photometric uncertainties were more than three standard deviations greater than the average uncertainty and then averaging a given night's observations. The average, min, and max of these nightly averages are what are given in Table 7.1. The type of each variable was determined by examining the amplitudes and shapes of the LCs in the context of the star's period and how regular it was from cycle to cycle. Some of the variable stars had been discovered by others and their official names are in Table 7.2. These names were found by searching the International Variable Star Index (VSX)[28] for variable stars near the coordinates of the variable stars found in this dataset. All the stars whose names are of the form "[WLR2013] ###" were discovered in Wehrung et al. (2013)[14] but have not been officially recognized yet as variable stars by GCVS.

All figures in this chapter have error bars and will adhere to the following color scheme: B data will always be shown in blue, V data in green, R data in magenta, I data in red, and $V - I$ data in black.

7.3.1 BG27 - IRAS 19050+0001 - ASASSN-V J190737.43+000609.1

IRAS 19050+0001 shows large variations in magnitude, 4.56 mag in V, with a periodicity that is regular from one cycle to the next (Figure 7.2). This paired with its period of 425 days, an extremely red color ($\langle V - I \rangle = 6.61$), and an amplitude in I of 2.92 mag make a strong case for this being a Mira type variable. There are no data in B due to how red the star is and how dim the B images are. At minimum V is approaching the detection threshold which is why the error bars suddenly become much larger. A distinguishing feature of many Mira type variables with periods greater than about 300 days is a relatively slow rise to maximum with a "bump" about halfway to maximum then a relatively fast drop back to minimum[29, 30]. The presence of this type of behavior is very evident in the phased LCs of IRAS 19050+0001 (Figure 7.3) and makes clear that IRAS 19050+0001 is a Mira type variable. IRAS 19050+0001 does show some clearly visible variation from cycle to cycle as is seen in the phased LC (Figure 7.3). This difference between cycles is probably caused either by slight differences in the photometric calibration from cycle to cycle, which could be more noticeable in very red stars, or from a second order physical effect like a 4500 day long secondary period or dust orbiting the star.

IRAS 19050+0001 was originally discovered in the IRAS survey as a bright infrared object. Its variability was originally discovered by Wehrung et al. (2013)[14]. However, they did not have data over long enough time scales to determine an accurate period or a certain identification of type. IRAS 19050+0001 appeared in the ASAS-SN survey[31] where it was found to have a period of 415 days with a V magnitude range of 14.82-15.8 mag. Their period is consistent with the one found in this study but their V magnitude range is significantly smaller, this is probably due the depth of their images; the ASAS-SN survey only goes to about 17 mag whereas this study goes to about 20 mag; this study also ranges from 2012 to 2017 and the ASAS-SN survey goes from 2014 to 2018, one year less.

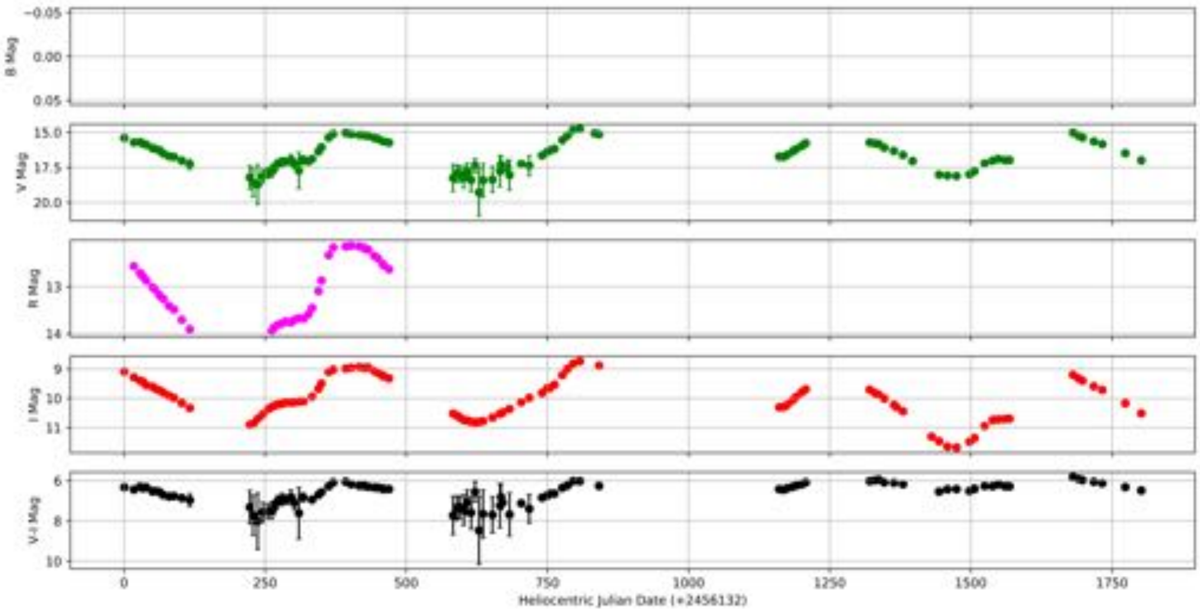

Figure 7.2: LC for IRAS 19050+0001. Note how regular the magnitudes are from one cycle to the next and how extremely red the star is. The point colors are defined at the beginning of Section 7.3.

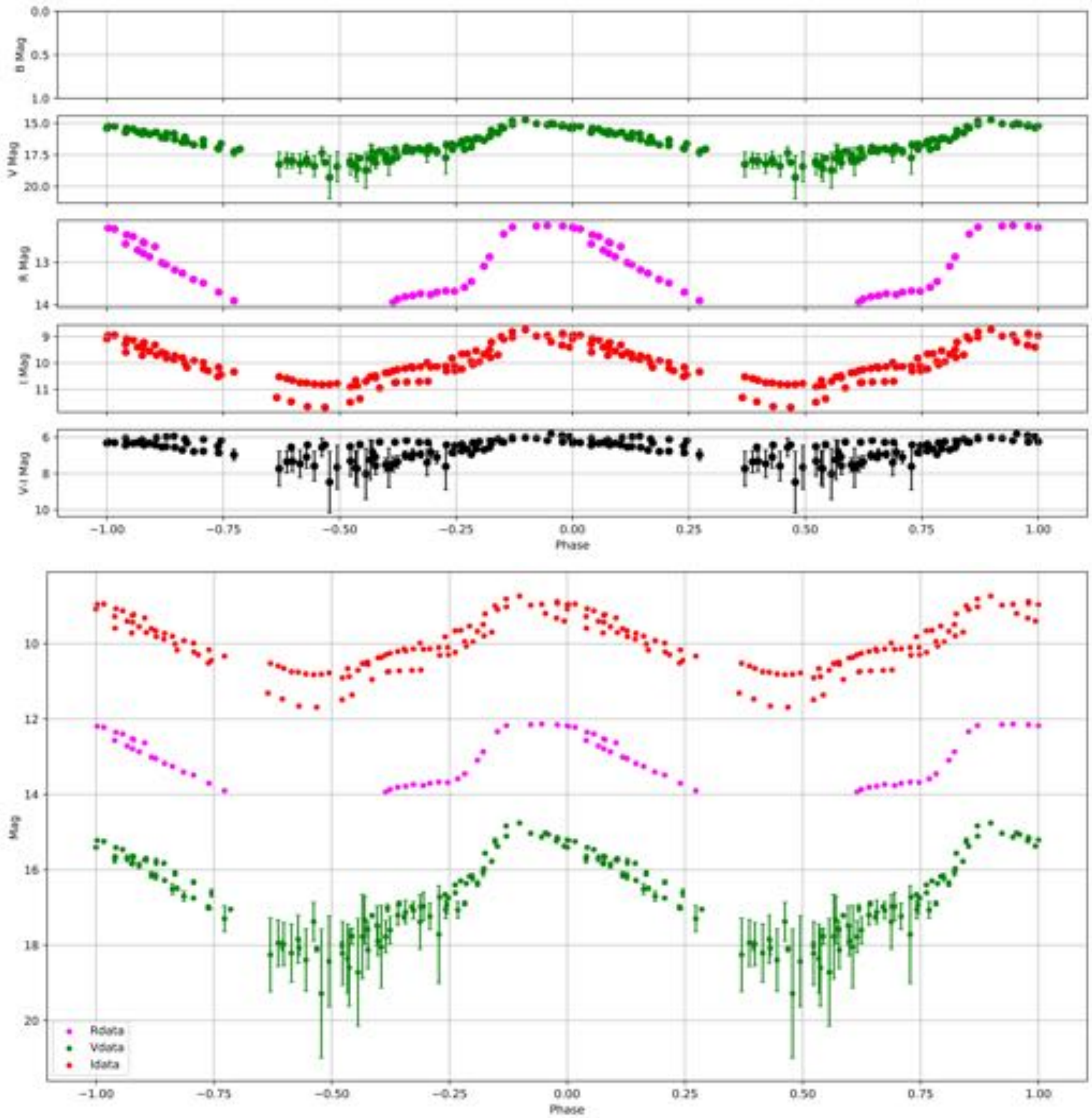

Figure 7.3: Phased light curves for IRAS 19050+0001 at a period of 425 days. **Top** shows each LC in separate plots and includes $V - I$. **Bottom** shows all LCs on the same plot. Note how little scatter there is throughout the phase and the small "bump" about halfway up to maximum. The point colors are defined at the beginning of Section 7.3.

7.3.2 BG26 - [WLR2013] 26

The variable star [WLR2013] 26 has two distinct periods at 70.3 and 67.1 days and very small amplitudes compared to IRAS 19050+0001 in each filter; the largest amplitude is in V and the amplitude there is only 0.75 mag. There were several other periods found by VSTAR with smaller powers. Some of these are probably real, since the two periods found here do not explain all of the variability, however it is unclear which of these higher order periods are real and which are aliases. The 70.3 and 67.1 day periods are most certainly real. The small changes in magnitude and less regular cycling compared to IRAS 19050+0001 are typical of a semi-regular variable star. Because of these two periods, phasing the LC (Figure 7.5) at its dominant period of 70.3 days still yields a graph that appears to have random scatter due to the strength of the secondary period. In this case there is a clearly defined primary period at 70.3 days so it is probably a type A semi-regular variable (SR)[4].

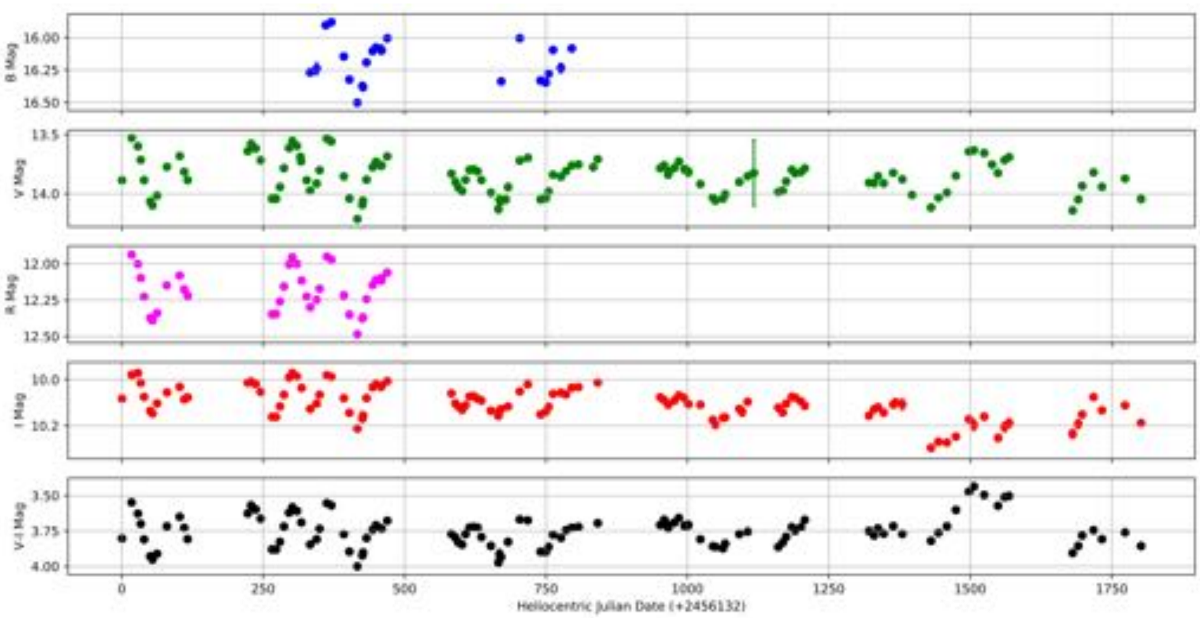

Figure 7.4: LC for [WLR2013] 26. Note the apparent irregularity caused by the two superimposed periods. The point colors are defined at the beginning of Section 7.3.

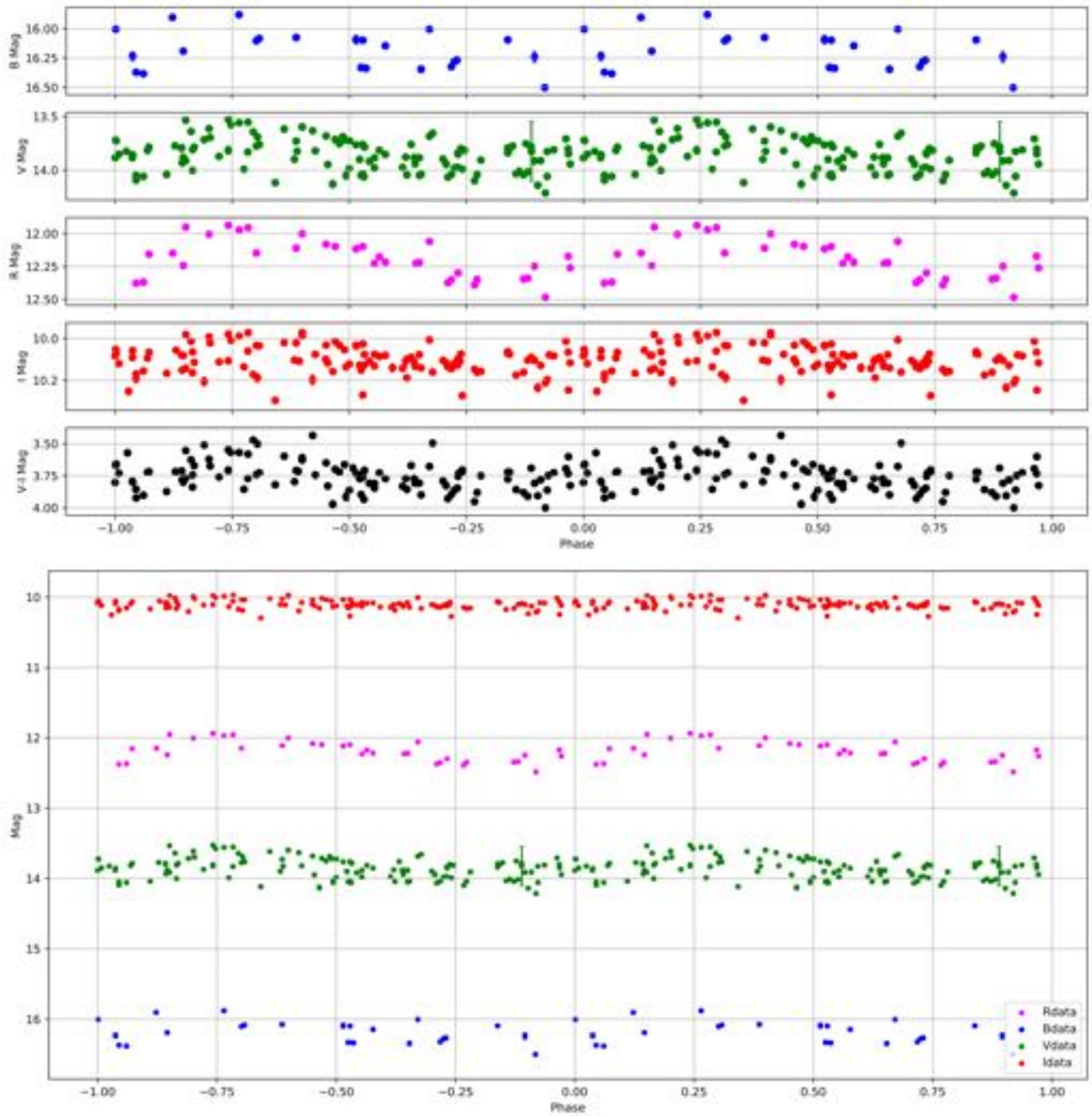

Figure 7.5: Phased LC for [WLR2013] 26 at a period of 70.3 days. **Top** shows each LC in separate plots and includes $V - I$. **Bottom** shows all LCs on the same plot. The point colors are defined at the beginning of Section 7.3.

7.3.3 BG244 - [WLR2013] 244

The star [WLR2013] 244, originally discovered by Wehrung et al. (2013), is a very interesting star. As seen in Figure 7.6, at around day 300 of this study it rapidly dims by a full magnitude in V and 0.5 mag in I. Then over the course of about 250 days it slowly returns to its original brightness and the dimming does not repeat again in the data. The asymmetry of the fall and rise prohibit any kind of eclipsing or rotational effect since those would be expected to be very symmetric and periodic. One type of star that does show this kind of variability are R Coronae Borealis variables (RCB). These stars are typically yellow supergiants and have rapid declines in brightness which are believed to be caused by carbon particles that are ejected from the star, condensing into dust rapidly and blocking a large portion of the emitted light[30]. These drops in brightness can be up to nine magnitudes and can occur periodically or not, seeing only a single event in five years of data is not atypical.

In addition to these dimming events, most RCB stars also show periodic variability on the order of a few tenths of a magnitude which often continues through an obscuration event. [WLR2013] 244 shows dipping and periodic variability that is consistent in magnitude with an RCB star but its period length and color are not. Typically RCB stars are of spectral type F, G, or K but de-reddening [WLR2013] 244's color returns $V - I = 2.89$, an M-type star. Some cooler RCBs are known but they are not common. The de-reddening value that was used was the same that used for V1835 Aql so at best it provides an estimate and at worst could be wildly incorrect for [WLR2013] 244 so the spectral type given here should not be considered definitive.

Most RCB stars also have periods of around 30 days compared to [WLR2013] 244's period of 63.4 days, however there is significant variation amongst RCB stars and it is not hard to imagine that an unusually cool RCB would also be larger and have a longer period. The 63.4 day period was found by eliminating all the data within the dimming event then performing a DFT on the remaining data. It appears probable that [WLR2013] 244 is an

R Coronae Borealis variable but if it is then it would be on the very cool, long-period, and low-amplitude end of the RCB spectrum. Determining a more accurate spectral type for [WLR2013] 244 via spectroscopy could provide additional evidence for or against the RCB hypothesis. Continued photometric observation are critical as these dimming events often repeat and finding a second one would support the RCB hypothesis.

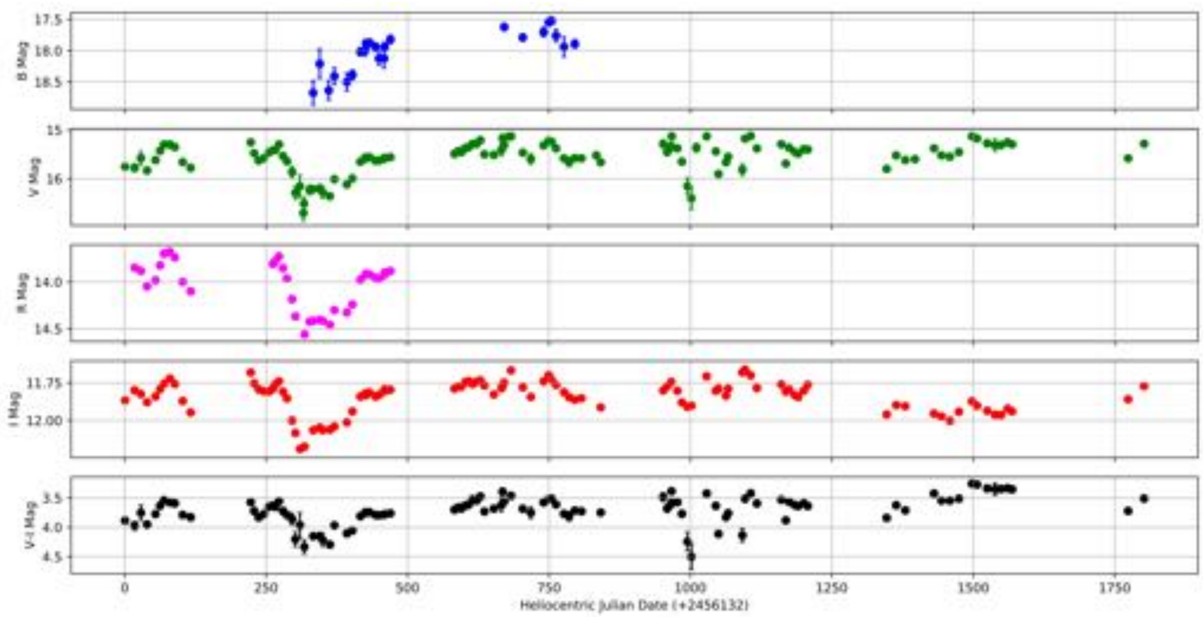

Figure 7.6: Light curve for [WLR2013] 244. Note the sudden drop in brightness and the slow return to normal brightness. The point colors are defined at the beginning of Section 7.3.

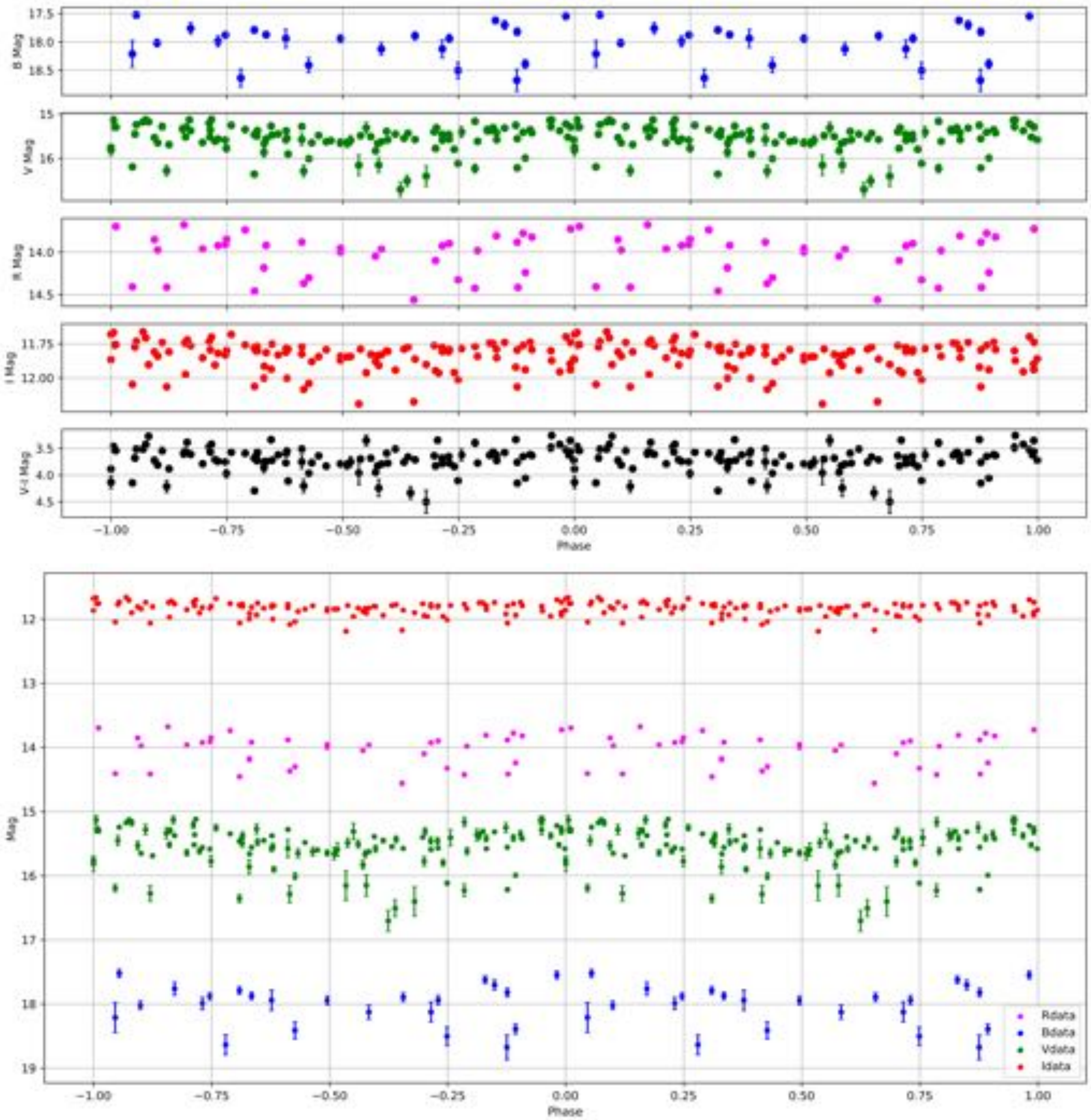

Figure 7.7: Phased LC for [WLR2013] 244 at a period of 68.2 days. **Top** shows each LC in separate plots and includes $V - I$. **Bottom** shows all LCs on the same plot. The point colors are defined at the beginning of Section 7.3.

7.3.4 P5-10

The light curves of P5-10 look like noise, which suggests that the period is below the sampling rate. Indeed, VSTAR found a distinct period at 15.121 days, near the lower limit that reliable periods could be found in the data. The 0.26 mag variations in V are too large to be an ellipsoidal variable[21] and the color is not constant enough for P5-10 to be entirely monochromatic. Determining the details is difficult due to how poorly sampled each period is. In this dataset observations were taken approximately every 14 days, on average sampling P5-10's 15.121 day period just once per period. Even with years worth of observations this kind of data is not well suited for determining periods this short.

P5-10 appears as an extremely blue star with a de-reddened $V - I$ value of -0.1, which is consistent with a B or A type star. This extreme blueness, combined with its position on the CMD and 15 day period, prohibit P5-10 from being most types of pulsating variables. P5-10's period is far too long to be any type of RR Lyrae variable or β Cephei and it is far too blue to be a Cepheid, δ Scuti, Type II Cepheid, or any kind of LPV/semi-regular variable. γ Doradus and α Cygni variables both have amplitudes around 0.1 mag, far smaller than the 0.26 mag amplitude that P5-10 has in V[30].

The variable star types that most accurately fit the color and period of of P5-10 are the very rare Luminous Blue Variables (LBV), also called S Doradus stars (SDor), and the more common Wolf-Rayet stars. Both of these types of star are evolved, massive, O and B type stars where the LBV phase is believed to lead into the final Wolf-Rayet phase before the star turns into a supernova[32, 30]. Both of these types of variables are extremely hot and can have periodic variations of a few tenths of a magnitude with periods anywhere between seconds and decades. Unfortunately, both of these types of variables are uniquely identified not by light curves but by their spectra. Without a spectrum of P5-10 it is impossible to determine if P5-10 is an LBV, a Wolf-Rayet star, or something else entirely. It is highly recommended that a 4000 Å to 7500 Å spectrum at medium resolution be taken of P5-10 to determine its exact classification and higher cadence photometric observations be taken to better determine P5-10's period.

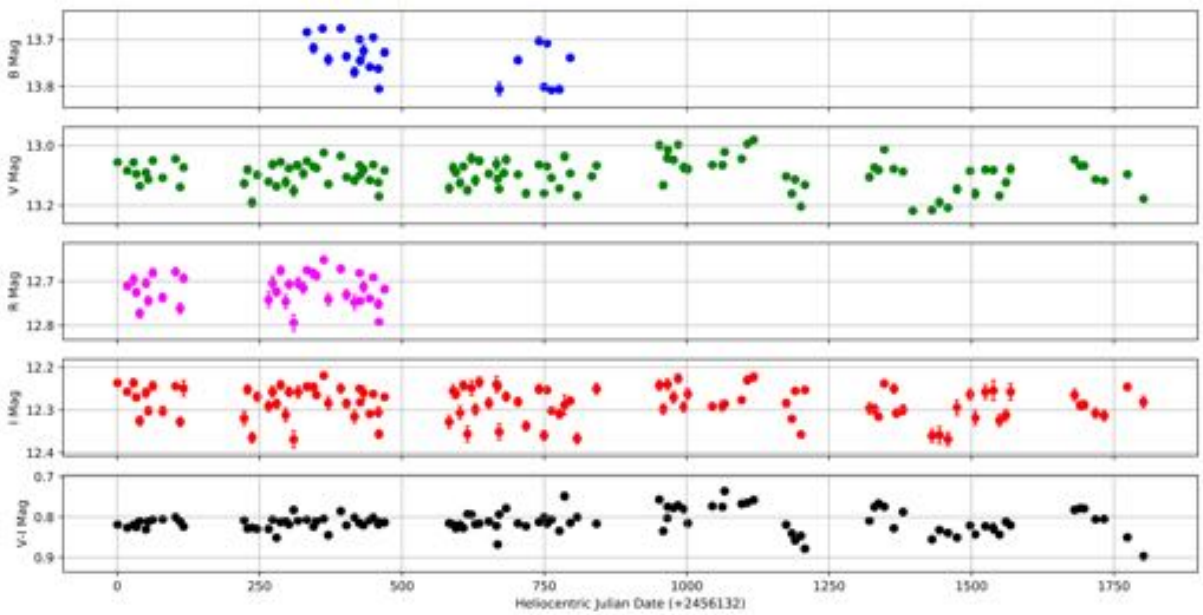

Figure 7.8: LC for P5-10. The point colors are defined at the beginning of Section 7.3.

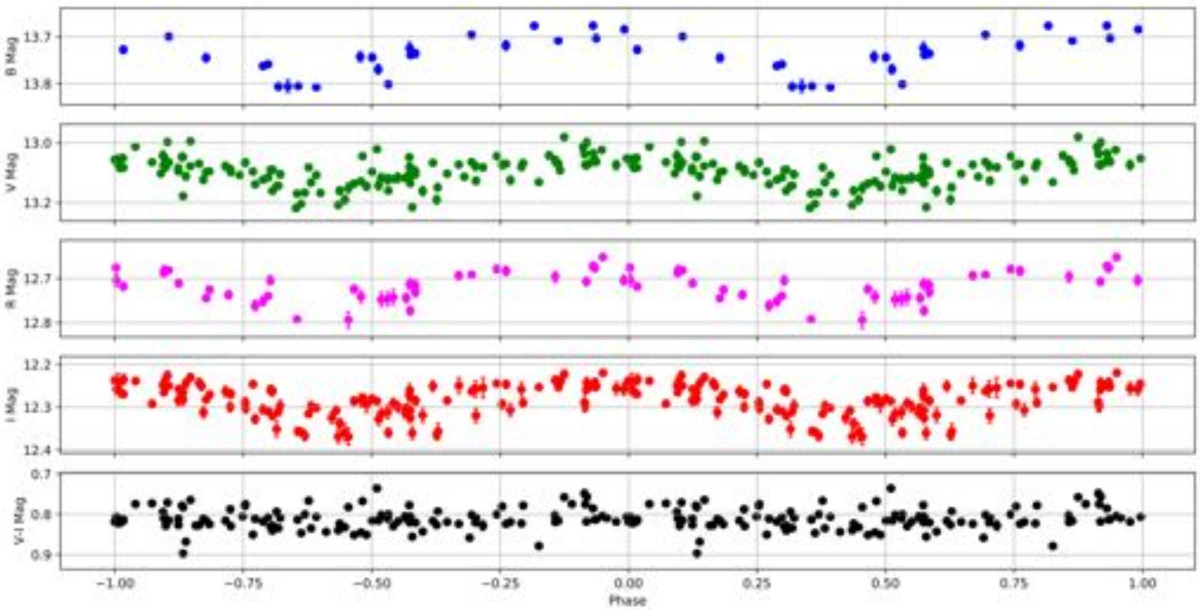

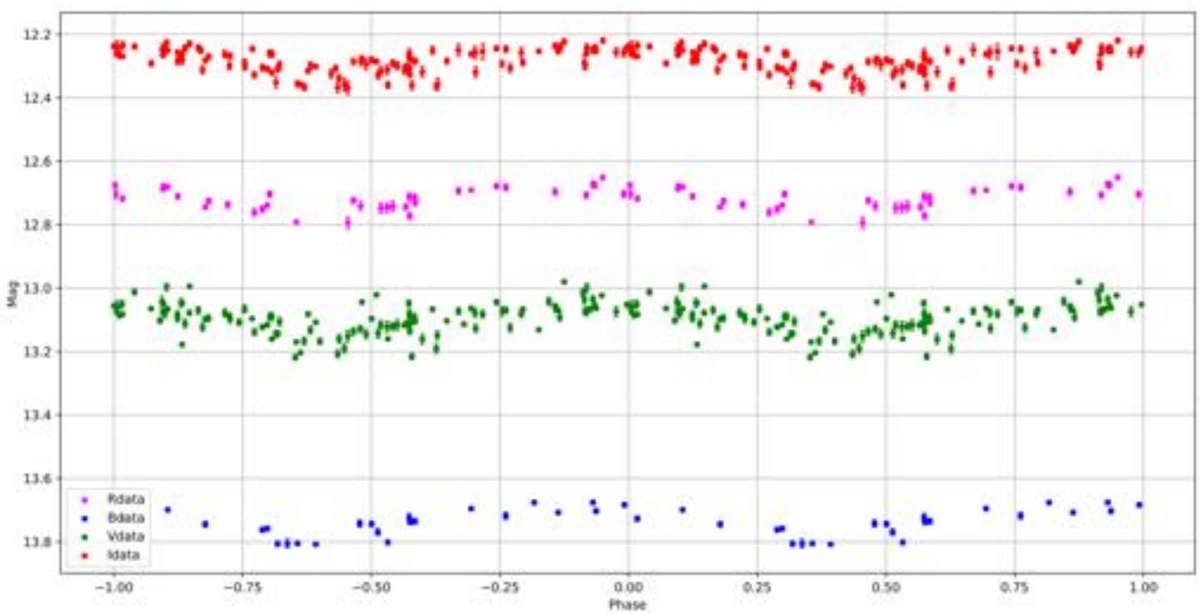

Figure 7.9: Phased LC for P5-10 at a period of 15.121 days. **Top** shows each LC in separate plots and includes $V - I$. **Bottom** shows all LCs on the same plot. The scatter is possibly due in part to the low sample rate and thus poorly constrained period. The point colors are defined at the beginning of Section 7.3.

7.3.5 P5-23

The star P5-23 is too blue to be a semi-regular variable or other LPV, though its 76.8 day period found with VSTAR is consistent with those types. Unlike these pulsating variables though, P5-23 has very little scatter in its phased light curves, Figure 7.11, which possibly indicates a rotational variable of some sort. P5-23's V amplitude of 0.41 mag is far too large to be an ellipsoidal variable and too symmetric to be from starspots. However, its light curve does resemble that of ζ Andromedae and AP Piscium, both of which are β Lyrae variables. β Lyrae variables are eclipsing variables which consist of a pair of main sequence or giant stars of similar sizes that are orbiting each other close enough to share an envelope or be semi-detached and so one star only completely eclipses the other vary briefly. This results in LCs that vary sinusoidally, even through eclipses. Typically they have minima of different depths but there are many β Lyrae variables with identical or virtually identical minima. If P5-23 is a β Lyrae variable then, given its de-reddened color of $V - I = 1.08$, it probably consists of a pair of red or yellow giants in a semi-detached orbit of 153.6 days, twice that of the 76.8 day orbit that VSTAR found. While it seems probable that P5-23 is a β Lyrae variable, time series spectrometry would have to be done both to determine the types of each star and to measure the radial velocity to determine if P5-23 is a binary system.

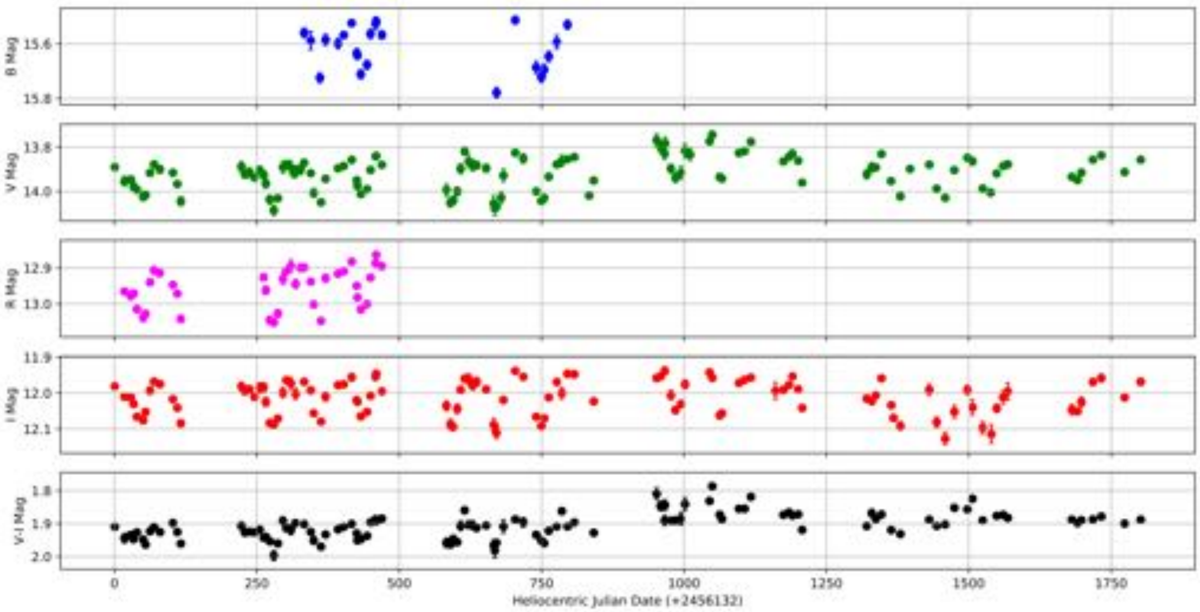

Figure 7.10: The point colors are defined at the beginning of Section 7.3.

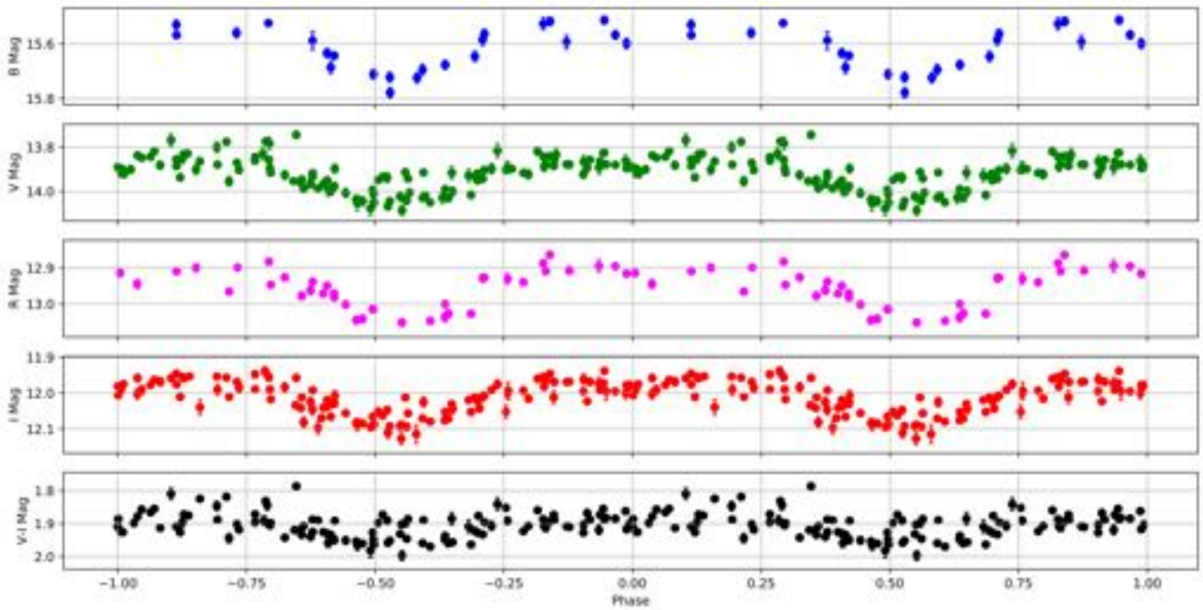

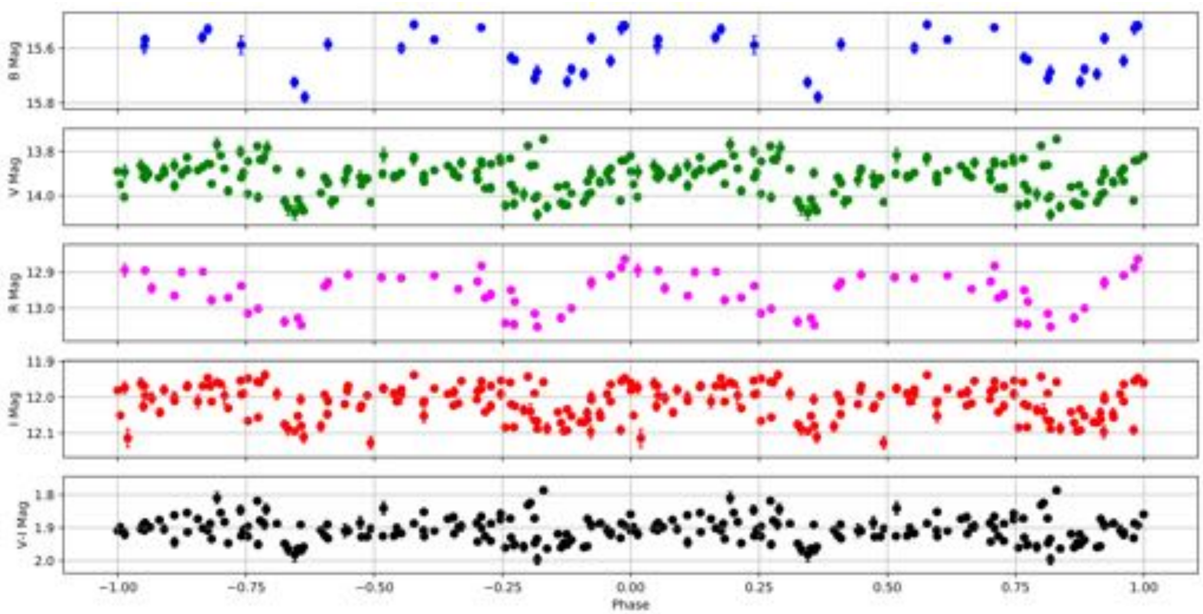

Figure 7.11: Phased LCs for P5-23. **Top** shows the LC phased at 76.8 days. **Bottom** shows the light curve phased at 153.6 days. The point colors are defined at the beginning of Section 7.3.

7.3.6 Notes on Interesting Variables

P5-85

The star P5-85 exhibits classic semi-regular behavior with a period of 374 days, small amplitudes, and stochastic variations on top of the 374 day periodicity. However, it also shows regular events where it dims by 0.5 to 1 magnitude in B, V, and R for a single night while brightening by about the same amount in I. P5-85 is in a cluster of 5-10 poorly resolved stars that center on BG1, the brightest star in the field. The sudden dimming and brightening events are probably caused by DAOPHOT blending multiple of these stars together. High-angular-resolution photometry of this part of the field would clarify the behavior of P5-85.

P5-120

The star P5-120 appears to be a semi-regular variable with a period of 46.3 days. It also has a long secondary period (LSP) at 488 days.

P5-238 and P5-1004

The star P5-238 has a de-reddened color of $V - I = 0.53$ which indicate that it could be an RR Lyrae type variable. To check this very short periods were searched for and P5-238 has a potential period at 0.3 days. This short period along with its de-reddened color of $V - I = 0.53$ indicate that P5-238 could be a type c RR Lyrae variable. However, a 0.3 day period is far below the roughly 10 day lower limit on periods that could be reliably determined with the data at hand so the period should be considered highly suspect. The star P5-1004 also has a de-reddened color of $V - I = 0.53$ and a short period at 0.6 days was found. Because of this P5-1004 could also be an RR Lyrae variable. High-cadence photometry of these stars is recommended to determine their types.

P5-356

VSTAR found two periods for P5-356 at 43.7 and 15.6 days. These short periods along with its de-reddened color of $V - I = 0.64$ indicate that P5-238 could be a Cepheid variable. However, in the P1_AU data set, with its poorer angular resolution, this star is indistinguishable from another star that is very close to it so all of the P1_AU data had to be thrown out. Even with the greater angular resolution available in the P5 data the star verges on being unresolved from the nearby star so any variability is suspect. High angular resolution photometry of this part of the field would clarify the behavior of P5-356.

P1 stars

All of the stars with IDs "P1-XXXX" are observed only in the P1_AU dataset, which only covers about 130 days. As a result the variable type stars could not be positively identified. P1-154, 270, 358, and 451 have been tentatively classified as slow irregular variables (Lb) whereas the variability of P1-1380 and 1383 could not be determined definitely and so they have been labeled as suspected variables (SV).

Table 7.1: Variable Stars in the Field-of-View

Stars marked with an asterisk have official names which can be found in Table 7.2.

SV indicates suspected variable.

ID	RA	Dec	$\langle B \rangle$	B_{min}	B_{max}	$\langle V \rangle$	V_{min}	V_{max}	$\langle R \rangle$	R_{min}	R_{max}	$\langle I \rangle$	I_{min}	I_{max}	$\langle V-I \rangle$	Period	Type
BG1*	19:07:44.30	0:07:10.0	14.01	14.25	13.85	11.72	12.01	11.43	9.83	9.93	9.69	7.38	7.69	7.17	4.34	49.5	Lb
BG26*	19:07:55.10	0:05:30.0	16.19	16.53	15.85	13.85	14.22	13.47	12.18	12.49	11.93	10.10	10.30	9.97	3.75	70.1/67.4	SRa
BG27*	19:07:37.50	0:06:09.0				16.68	19.29	14.73	13.05	13.95	12.13	10.07	11.69	8.73	6.61	425	M
BG62*	19:07:42.40	0:02:22.0	17.19	17.57	16.77	14.88	16.38	14.14	13.04	13.41	12.69	10.78	11.08	10.57	4.10	62.0	SRa
BG85*	19:07:30.22	-0:02:51.2				14.94	15.18	14.75				10.98	11.09	10.89	3.96	??	Lb?
BG132*	19:07:10.50	-0:01:53.6				15.46	15.60	15.32				11.19	11.28	11.09	4.27	103?	Lb?
BG244*	19:07:25.10	0:00:59.0	18.03	18.85	17.38	15.56	16.86	15.08	14.07	14.58	13.67	11.84	12.22	11.65	3.72	63.4/447	SR/RCB?
BG255*	19:07:48.50	0:05:32.0	18.06	18.52	17.77	15.76	16.18	15.52	14.10	14.22	13.90	12.06	12.29	11.95	3.70	45.5?	SRb
BG419*	19:07:17.17	0:00:40.2				17.40	18.24	16.57				13.06	13.47	12.48	4.34	209?	SR?
P5-10	19:07:55.27	-0:01:19.4	13.73	13.83	13.65	13.10	13.23	12.97	12.71	12.80	12.63	12.28	12.40	12.21	0.82	15.12	WR?/SDOR?
P5-23	19:07:48.67	-0:01:07.5	15.61	15.78	15.49	13.92	14.11	13.70	12.96	13.06	12.86	12.01	12.14	11.92	1.91	78.6	SR?
P5-30	19:07:20.39	0:01:26.7	16.42	16.56	16.30	14.27	14.60	14.19	12.94	13.02	12.88	11.47	11.59	11.38	2.80	19.8	SR
P5-75	19:07:42.72	0:04:40.5	17.80	18.01	17.60	15.43	15.82	15.14	13.72	13.92	13.52	11.52	11.73	11.42	3.91	42/300	SR
P5-85	19:07:44.59	0:07:13.8	16.82	17.41	16.65	15.17	16.31	14.80	14.27	15.41	13.97	12.78	14.90	11.61	2.39	374	SR?
P5-108	19:07:42.57	-0:02:04.8				16.32	17.22	15.72	14.60	14.72	13.95	12.61	12.83	12.47	3.71	336	SR
P5-116	19:07:44.95	0:04:05.3				16.77	17.51	16.19	14.72	14.89	14.48	12.21	12.54	12.03	4.56	38.1	SR
P5-120	19:07:23.13	0:07:17.3	18.32	18.72	17.99	16.05	16.88	14.36	14.39	14.62	14.20	12.36	12.60	12.22	3.69	46.3/488	SR/LSP
P5-132	19:07:42.19	0:02:23.8	17.12	17.32	16.96	15.52	16.98	15.10	14.58	14.81	14.40	13.71	14.43	13.36	1.81	178	SV
P5-157	19:07:27.11	0:03:21.9	18.84	19.45	18.18	16.65	17.41	16.02	14.77	14.91	14.65	12.30	12.56	12.18	4.35	322/169	Lb?
P5-193	19:07:38.18	0:04:24.1	18.72	19.17	18.33	16.36	16.73	16.04	14.89	15.04	14.77	13.24	13.38	13.16	3.12	57.3?	Lb?
P5-215	19:07:56.60	0:02:27.1	18.71	19.47	18.31	16.39	16.90	15.91	15.07	15.24	14.93	13.64	13.78	13.54	2.75	190	SV
P5-238	19:07:22.34	0:06:54.0	17.30	17.67	17.08	16.23	16.63	15.69	15.57	15.90	15.25	14.87	15.26	14.58	1.36	0.3	RRc?
P5-277	19:07:34.09	0:06:10.0	18.03	18.52	17.64	16.44	17.00	15.99	15.45	15.74	15.22	14.61	14.95	14.38	1.83	70	SR?
P5-356	19:07:52.75	0:07:13.7	17.66	18.02	17.23	16.54	17.14	15.96	15.89	16.22	15.71	15.07	15.45	14.39	1.47	43.7/15.6	CEP?
P5-1004	19:07:26.66	-0:00:11.2	18.82	20.18	17.62	17.68	18.61	16.57	17.01	17.75	16.42	16.28	17.01	15.51	1.40	0.6	RRab?
P1-154	19:08:06.59	-0:03:42.7				15.19	15.43	14.96				11.23	11.35	11.08	3.96	73.9/627?	Lb?
P1-270*	19:07:26.77	-0:03:47.8				15.37	16.51	14.83				12.10	12.66	11.82	3.27	70.2?	Lb?
P1-358	19:07:36.81	0:14:03.7				16.36	16.57	16.14				11.85	11.96	11.70	4.51	126?	Lb?
P1-451	19:07:42.22	0:08:26.0				17.12	17.76	16.79				11.77	12.13	11.56	5.35	14.2/74.9?	Lb?
P1-1380	19:07:48.07	-0:05:47.7				16.13	16.87	15.90				15.05	15.74	14.81	1.08	621?	SV
P1-1383	19:07:28.35	-0:03:29.7				16.32	16.55	16.02				14.57	14.93	14.32	1.75	209?	SV

Table 7.2: ID to Official Names

ID	Name
BG1	ASAS 190744+0007.1
BG26	[WLR2013] 26
BG62	[WLR2013] 62
BG85	[WLR2013] 85
BG132	[WLR2013] 132
BG244	[WLR2013] 244
BG27	IRAS 19050+0001 ASASSN-V J190737.43+000609.1
BG255	[WLR2013] 255
BG419	[WLR2013] 419
P1-270	ASASSN-V J190726.81-000347.7

7.4 Summary

Searching the field near V1835 Aql for variable stars led to the discovery of 31 other variable stars. Most of the other variable stars are LPVs of some sort: one Mira variable, nine slow irregular variables (Lb), and 13 semi-regular variables. Half of the remaining eight stars are suspected variables. Their variability is undetermined either because their amplitudes are so small or because they only appear in the P1_AU dataset and so only a small fraction of their period could be observed. Three shorter period, blue variables were also found and marked as potential Cepheids or RR Lyrae stars but their periods are so short no positive identification could be made. The most interesting find was P5-10, a potential Luminous Blue Variable or Wolf-Rayet star.

CHAPTER 8
CONCLUSION

This study examined the symbiotic nova V1835 Aql and the surrounding star field for five years. The field was imaged every two weeks with 2-4 different filters. The SKYNET system was used to automatically provide the bias, dark, and flat calibrations for the observations. Photometry was done by DAOPHOT using PSF fitting photometry. The instrumental magnitudes provided by DAOPHOT were calibrated to the standard system using secondary standards provided by Wehrung et al. (2013) [14] and APASS [17].

The long temporal baseline of these observations has led to significant discoveries about the nature of V1835 Aql. Bond & Kasliwal (2012)[2] showed that V1835 Aql is a symbiotic star by observing the spectral line at 6825 Å, which is unique to symbiotic stars. This study has shown that V1835 Aql has an orbital period of 419 $\pm$ 12 days. Using this period to determine upper and lower bounds for orbital separation yields an orbital separation of 1.0 to 1.9 AU with a typical value of 1.6 AU[24]. Additionally, the variability of V1835 Aql can be explained entirely by the red giant interacting with its companion star through two mechanisms. The first is the ellipsoidal variability from tidal distortion, and the second, larger effect is the polychromatism of the photosphere caused by asymmetric heating of the M3/M4 spectral type red giant star. This is the simplest explanation that fits the observed variability and so is presented with a high degree of confidence. V1835 Aql is consistent with an S-type symbiotic star due to the strong Hα lines and lack of mid infrared lines in its optical spectra[14, 2].

While this study has been able to determine several properties of the system it has not been able to determine if the companion star is a white dwarf or a neutron star. It also has been unable to determine if there is any active accretion of matter by the compact star. UV and X-ray spectra should be able to determine the identity of the compact star and the accretion behavior of the system. High cadence (2-3 images per minute) photometric observations in UV and X-ray might show flickering from an accretion disk which would indicate if there is any active accretion and if so, the rate of that accretion[33]. Previous visible and IR spectra of V1835 Aql have been taken at random phases and so do not show anything definitive about the orbital dynamics of the system or the polychromatism discovered in this study. Visible and IR spectra taken regularly throughout the orbital cycle could shed significant light on the orbital characteristics of V1835 Aql and provide more accurate measurements of the temperature differential across the surface of the red giant. Time series K band photometry could also provide confirmation of ellipsoidal variability.

In addition to V1835 Aql, 31 other variable stars were found in the field-of-view, 21 of which are new discoveries. These stars consist primarily of semi-regular variables (13 in total) but there are also a Mira, nine slow irregular variables, one suspected Cepheid, two suspected RR Lyrae stars, one suspected Luminous Blue Variable or Wolf-Rayet star. Four of the variable stars discovered have periods that are too short to be well sampled in this study, so are listed as suspected variables (SV) in Table 7.1. Determining the properties of the shorter period variable stars could be done by taking nightly images for 6-8 weeks for the stars with < 20 day periods and a few nights of continuous observing for stars with periods < 1 day. P5-10 is of especial interest as a Luminous Blue Variable or Wolf-Rayet star candidate. Spectra of P5-10 would be required to accurately determine which it is or to eliminate both possibilities.

REFERENCES

[1] D. B. Williams. NSV 11749: Slow nova or FU Ori variable? *Journal of the American Association of Variable Star Observers (JAAVSO)*, 34:43–45, 2005.

[2] H. E. Bond and M.M. Kasliwal. NSV 11749: Symbiotic nova, not a born-again red giant. *Publications of the Astronomical Society of the Pacific*, 124(922), 2012.

[3] S. J. Smartt. Observational constraints on the progenitors of core-collapse supernovae: the case for missing high-mass stars. *Publications of the Astronomical Society of Australia*, 32, 2015.

[4] N. N. Samus, E. V. Kazarovets, O. V. Durlevich, N. N. Kireeva, and E. N. Pastukhova. General catalogue of variable stars: Version GCVS 5.1. *Astronomy Reports*, 61(1):80–88, 2017.

[5] U. Munari, B. F. Yudin, O. G. Taranova, G. Massone, F. Marang, G. Roberts, H. Winkler, and P. A. Whitelock. UBVRI-JHKL photometric catalogue of symbiotic stars. *Astronomy and Astrophysics Supplement Series*, 93:383–390, 1992.

[6] U. Munari and A. Renzini. Are symbiotic stars the precursors of Type Ia supernovae? *The Astrophysical Journal*, 397:L87–L90, 1992.

[7] K. Belczyński, J. Mikołajewska, U. Munari, R. J. Ivison, and M. Friedjung. A catalogue of symbiotic stars. *Astronomy and Astrophysics Supplement Series*, 146(3):407–435, 2000.

[8] B. L. Webster and D. A. Allen. Symbiotic stars and dust. *Monthly Notices of the Royal Astronomical Society*, 171(1):171–180, 1975.

[9] R. Angeloni, C. E. Ferreira Lopes, N. Masetti, F. Di Mille, P. Pietrukowicz, A. Udalski, B. E. Schaefer, P. Parisi, R. Landi, C. Navarrete, M. Catelan, T. H. Puzia, and D. Guzman. Symbiotic stars in OGLE data - I. Large Magellanic Cloud systems. *Monthly Notices of the Royal Astronomical Society*, 438(1):35–48, 2014.

[10] L. Hartmann and S. J. Kenyon. The FU Orionis phenomenon. *Annual Review of Astronomy and Astrophysics*, 34(1):207–240, 1996.

[11] I. Iben Jr. On the frequency of planetary nebula nuclei powered by helium burning and on the frequency of white dwarfs with hydrogen-deficient atmospheres. *The Astrophysical Journal*, 277:333–354, 1984.

[12] D. Schönberner. Asymptotic giant branch evolution with steady mass loss. *Astronomy and Astrophysics*, 79:108–114, 1979.

[13] J. E. Grindlay, J. Hong, P. Zhao, S. Laycock, M. van den Berg, X. Koenig, E. M. Schlegel, H. N. Cohn, P. M. Lugger, and A. B. Rogel. Chandra multiwavelength plane (ChaMPlane) Survey: An introduction. *The Astrophysical Journal*, 635(2):920, 2005.

[14] M. Wehrung, A. Layden, A. Rogel, D. Reichart, K. Ivarsen, J. Haislip, M. Nysewander, and A. LaCluyze. Time-series photometry of the symbiotic nova NSV 11749 and new variable stars in Aquila. *Information Bulletin on Variable Stars*, 6071, 2013.

[15] D. Reichart, M. Nysewander, J. Moran, J. Bartelme, M. Bayliss, A. Foster, J. C. Clemens, P. Price, C. Evans, J. Salmonson, S. Trammell, B. Carney, J. Keohane, and R. Gotwals. PROMPT: panchromatic robotic optical monitoring and polarimetry telescopes. *arXiv preprint astro-ph/0502429*, 2005.

[16] P. B. Stetson. DAOPHOT: A computer program for crowded-field stellar photometry. *Publications of the Astronomical Society of the Pacific*, 99(613):191, 1987.

[17] A. Henden and U. Munari. The APASS all-sky, multi-epoch BVgri photometric survey. *Contrib. Astron. Obs. Skalnate Pleso*, 43:518–522, 2014.

[18] A. A. Henden, M. Templeton, D. Terrell, T. C. Smith, S. Levine, and D. Welch. VizieR online data catalog: AAVSO Photometric All Sky Survey (APASS) DR9. *VizieR Online Data Catalog*, 2336, 2016.

[19] A. U. Landolt. Broadband UBVRI photometry of the Baldwin-Stone southern hemisphere spectrophotometric standards. *The Astronomical Journal*, 104:372–376, 1992.

[20] A. C. Layden, T. B. Bowes, D. L. Welch, and T. M. A. Webb. Variable stars in metal-rich globular clusters. II. NGC 6316. *The Astronomical Journal*, 126(1):255, 2003.

[21] I. Soszynski, A. Udalski, M. Kubiak, M. K. Szymanski, G. Pietrzynski, K. Zebrun, O. Szewczyk, Ł. Wyrzykowski, and W. A. Dziembowski. The optical gravitational lensing experiment. ellipsoidal variability of red giants in the large magellanic cloud. *Acta Astronomica*, 54, 2004.

[22] R. E. Wilson. Accuracy and efficiency in the binary star reflection effect. *The Astrophysical Journal*, 356:613–622, 1990.

[23] P. J. Amado and P. B. Byrne. Effective temperature-colour and surface brightness-colour relationships for the latest-type stars. *Irish Astronomical Journal*, 23, 1996.

[24] J. Mikolajewska. Orbital and stellar parameters of Symbiotic Stars. *ASP Conference Series*, 303, 2003.

[25] R. E. Wilson and E. J. Devinney. Realization of accurate close-binary light curves: application to MR Cygni. *The Astrophysical Journal*, 166:605, 1971.

[26] A. Prša, K. E. Conroy, M. Horvat, H. Pablo, A. Kochoska, S. Bloemen, J Giammarco, K. M. Hambleton, and P. Degroote. Physics of eclipsing binaries. ii. toward the increased model fidelity. *The Astrophysical Journal Supplement Series*, 227(2):29, 2016.

[27] D. L. Welch and P. B. Stetson. Robust variable star detection techniques suitable for automated searches-new results for NGC 1866. *The Astronomical Journal*, 105:1813–1821, 1993.

[28] C. L. Watson. The international variable star index (VSX). In *Society for Astronomical Sciences Annual Symposium*, volume 25, page 47, 2006.

[29] J. A. Mattei. Introducing Mira variables. *Journal of the American Association of Variable Star Observers (JAAVSO)*, 25:57–62, 1997.

[30] C. Sterken and C. Jaschek. Light curves of variable stars, 1996.

[31] T. Jayasinghe, C. S. Kochanek, K. Z. Stanek, B. J. Shappee, T. W-S. Holoien, T. A. Thompson, J. L. Prieto, Subo Dong, M. Pawlak, J. V. Shields, G. Pojmanski, S. Otero, C. A. Britt, and D. Will. The ASAS-SN catalog of variable stars I: The serendipitous survey. *Monthly Notices of the Royal Astronomical Society*, 2018.

[32] A. van der Hucht Karel. The VIIth catalogue of galactic wolf-rayet stars. *New Astronomy Reviews*, 45(3):135 – 232, 2001.

[33] J. L. Sokoloski, L. Bildsten, and W. C. G. Ho. A search for rapid photometric variability in symbiotic binaries. *Monthly Notices of the Royal Astronomical Society*, 326(2):553–577, 2001.

[34] M. M. Miller Bertolami, R. D. Rohrmann, A. Granada, and L. G. Althaus. NSV 11749, an elder sibling of the born-again stars V605 Aql and V4334 Sgr? *The Astrophysical Journal*, 743(2), 2011.

[35] S. J. Kenyon and R. F. Webbink. The nature of symbiotic stars. *The Astrophysical Journal*, 279:252–283, 1984.

[36] J. Mikołajewska, N. Caldwell, and M. M. Shara. First detection and characterization of symbiotic stars in M31. *Monthly Notices of the Royal Astronomical Society*, 444(1):586–599, 2014.

[37] J. Mikołajewska, M. M. Shara, N. Caldwell, K. Drozd, K. Iłkiewicz, and D. Zurek.

Symbiotic stars in the local group of galaxies. *EAS Publications Series*, 71:199–204, 2015.

[38] H. M. Schmid. Identification of the emission bands at $\lambda\lambda$6830, 7088. *Astronomy and Astrophysics*, 211:L31–L34, 1989.

[39] E. A. Kolotilov, V. I. Shenavrin, S. Yu. Shugarov, and B. F. Yudin. UBVJHKLM photometry of the symbiotic Mira V407 Cyg in 1998–2002. *Astronomy Reports*, 47(9):777–788, 2003.

[40] A. Henden and U. Munari. $UBV(RI)_C$ photometric comparison sequences for symbiotic stars. *Astronomy and Astrophysics Supplement Series*, 143(2):343–355, 2000.

[41] S. Hümmerich, S. Otero, P. Tisserand, and K. Bernhard. The curious case of ASAS J174600-2321.3: an eclipsing symbiotic nova in outburst? *Journal of the American Association of Variable Star Observers (JAAVSO)*, 43, 2015.

[42] U. Munari, M. Rejkuba, M. Hazen, J. Mattei, E. Schweitzer, R. Luthardt, S. Shugarov, B. F. Yudin, A. A. Popova, P. V. Chugainov, G. Sostero, and A. Lepardo. The symbiotic star YY Herculis. I. photometric history over 1890-1996. *Astronomy and Astrophysics*, 323:113–120, 1997.

[43] L. Formiggini and E. M. Leibowitz. Three periodicities in a 98-year light curve of the symbiotic star Z Andromedae. *Astronomy and Astrophysics*, 292:534–542, 1994.

[44] L. Leedjärv. Cataclysmic variables and symbiotic stars–challenging targets for small telescopes. *Contrib. Astron. Obs. Skalnaté Pleso*, 43:282–289, 2013.

[45] E. J. Michaels. A photometric study of the eclipsing binary QT Ursae Majoris. *Journal of the American Association of Variable Star Observers (JAAVSO)*, 45:133, 2017.

[46] D. A. Leahy and J. C. Leahy. A calculator for Roche lobe properties. *Computational Astrophysics and Cosmology*, 2(1):4, 2015.

APPENDIX A

CALIBRATION PROGRAM

A.1 Overview of Program

To implement the conversion from the instrumental magnitudes provided by DAOPHOT and ALLFRAME to standard magnitudes, described in Chapter 3, I wrote a program in Python. This program consists of four separate `.py` files and over 800 lines of code. Since this is the most complicated piece of code I wrote during my research I have presented it here.

The format of the code is as follows: `instr2standardmag.py` (Section A.3) converts the magnitudes in the `.raw` file output by DAOMASTER so that we have an average standard magnitude for each star in the data set. The `.raw` file contains the average instrumental magnitudes for each star in each filter. This step outputs a `.std` file that is used to calibrate the magnitudes on an image-by-image basis. The `daomaster_Data_Reducer.py` (Section A.4) program acts primarily as a controller: it sets all the file paths and various settings that the calibration needs, then uses the functions in `file_reader.py` (Section A.5) to read the various files into NumPy arrays. NumPy is a Python library which provides tools for complex numerical computing. It is used here to simplify much of the programming and decrease execution time. The `daomaster_Data_Reducer.py` program then reads the `.cor` files in parallel using the `joblib` library. The `.cor` files contain the instrumental magnitudes for each star in each image, but only for a single filter, which is why multiple `.cor` files must be read. Parallelizing reading the `.cor` files was done to decrease the time it takes to read and organize the files into useful formats and reduced the total runtime of the program by about a factor of two. After the program finishes reading and formatting all the files it uses the functions inside of `daom_analyzer.py` (Section A.6) to convert all of the data onto a standard ID system, calibrate to the standard magnitudes (using the method discussed in Chapter 4), and stitch the data from the various filters together into a NumPy structured array. The final structured array for each dataset is then saved in binary format as a `.npy` file which can easily be read by other python programs.

Detailed documentation on what each part of the program does can be found in the comments and docstrings within the code. Minor modifications to the format of the code have been made to improve readability when typset by LaTeX.

A.2 Dependencies

The Python version, libraries, and version number of those libraries that were used are listed in Table A.1. The listed libraries might have their own dependencies which are not listed and libraries that are in the standard install of Python 3.6.3 are also not listed. While the program might work with older or newer versions it is not guaranteed and it is certainly not compatible with any version of Python 2 or earlier.

Table A.1: Software Versions

Software	Version
Python	3.6.3
NumPy	1.13.3
Astropy	2.0.2
Joblib	0.11

A.3 `instr2standardmag.py`

```
'''
==========================================================================

 This program takes the .raw file from daomaster and applies a 1 or 2
```

```
 parameter fit to the magnitudes to convert from instrumental magnitudes
 to standard magnitudes.  It is generalized to run on a .raw file with any
 even number of magnitude-error pairs.  NOTE: this function assumes
 that each pair of magnitdues is ordered v,i,v,i etc since it's uses the
 following system of equations to solve for V and I
 V = v - c_0 - c_1(V-I)
 I = i - c'_0 - c'_1(V-I)
===========================================================================

'''

import numpy as np

#=====================================================================
# This section simply creates the settings and variables that the rest of
# this program will need.  Settings for previous data sets can be found
# commented out at the end
# NOTE: ZO and FO always stand for 'zero order' and 'first order'
# respectively
#=====================================================================
#path to the .raw file
rawpath = '/Users/bob/Desktop/masters_research/Analyzed_Data/P5_AA/daom
                                     files/daom_VR/daom_VRalf.raw'

# order of fit. options are '0','1', or '01' which does both and generate
# separate files. dtype='str'
fittype = '1'

# coefs. ZeroOrder is the ordered list of the Zero order coefs, FirstOrder
# is the ordered list of the zero and first order fits for the two
# parameter fit in each vi pair, aka [c_0, c_1, c'_0, c'_1].  If only
# using one type of fit make the other list empty
```

```
Z0coefs = []#[-7.427724E-1, 1.130149E0, -7.645665E-1, 1.312145E0]
F0coefs = np.array([[-3.190328E-1,5.907696E-2,3.597813E-1,9.368310E-2]])

# output filepaths, if only using one fite type just make the other a
# blank string
Z0path = ''#'/users/bob/desktop/comparison_zeroth.std'
F0path =  '/Users/bob/Desktop/masters_research/Analyzed_Data/P5_AA/daom
                                    files/daom_VR/daom_VRalf_first.std'

#=====================================================================
# End Settings section
#=====================================================================

def Writer(VI,order):
    '''writes the given data in the same format as the original .raw file
                                            '''

    # Read the header of the .raw file and make it a single string
    with open(rawpath) as rawfile:
        head = [next(rawfile) for x in range(3)]
    head = ''.join(head)

    # Determine which destination path to use
    if order == '0':
        path = Z0path
    elif order == '1':
        path = F0path
    else:
        print('Error in determing the order of fit for Writer function')

    # saves the file in the same format as the original .raw file
    form = '%6d %8.3f %8.3f  %7.4f  %7.4f  %7.4f  %7.4f  %7.4f  %7.4f'
```

```
    np.savetxt(path,VI,fmt=form, header=head, comments='')



def ZeroOrderCorrector(vi):
    '''determines the correction to the magnitude to the zeroth order and
    sends the new VI to the Writer function'''
    # copy vi data for editing
    VI = np.array(vi, copy=True)

    # determine which columns have the magnitudes
    columns = []
    i=3
    while len(columns) < len(ZOcoefs):
        columns.append(i)
        i+=2

    # iterate through each column then row and if the object is in the
    # field (aka not 999) then apply the zero point correction
    for i,col in enumerate(columns):
        for j in range(len(VI[:,col])):
            if VI[j,col] < 90.:
                VI[j,col] = VI[j,col]-ZOcoefs[i]

    #now write the file
    Writer(VI,'0')



def FirstOrderCorrector(vi):
    '''determines the correction to the magnitude to the first order and
    sends the new VI to the Writer function'''
    # copy vi data for editing
    VI = np.array(vi, copy=True)
```

```
    # do the calculatrions, pairnum is the number of the vi set we're
    # currently on, paircoefs is the set of coefs for that vi pair
    for pairnum,paircoefs in enumerate(FOcoefs):
        # generate the matrix of coefs
        coefmatrix = np.array([[1+paircoefs[1],-paircoefs[1]], [paircoefs[
                                                     3], 1-paircoefs[3]]])

        # Grab just the V and I data from that pair
        V = VI[:,pairnum*4+3]
        I = VI[:,pairnum*4+3+2]

        # iterate through V and I and if the object exists then use
        # linalg.solve to solve the system of equations
        for i in range(len(V)):
            if (V[i]<90.) and (I[i]<90.):
                constants =np.array([V[i]-paircoefs[0],I[i]-paircoefs[2]])
                [V[i], I[i]] = np.linalg.solve(coefmatrix,constants)

    #now write the file
    Writer(VI,'1')


#=====================================================================
# Controller
#=====================================================================
# Read the .raw file,
vi = np.loadtxt(rawpath, skiprows=3)

# Decide to do Zero order correct, First order correction, or both
if '0' in fittype:
    ZeroOrderCorrector(vi)
```

```
if '1' in fittype:
    FirstOrderCorrector(vi)



# P5_AA SETTINGS
#==================================================================
##path to the .raw file
#rawpath = '/Users/bob/Desktop/masters_research/Analyzed_Data/P5_AA/
                                     daom_VI/daom_VIalf.raw'
#
## order of fit. options are '0','1', or '01' which does both and generate
## separate files. dtype='str'
#fittype = '1'
#
## coefs. ZeroOrder is the ordered list of the Zero order coefs,
## FirstOrder is the ordered list of the zero and first order fits
## for the two parameter fit in each vi pair, aka [c_0, c_1, c'_0, c'_1].
## If only using one type of fit make the other list empty
#ZOcoefs = []#[-7.427724E-1, 1.130149E0, -7.645665E-1, 1.312145E0]
#FOcoefs = np.array([ [-0.3152580425, 0.02406, 0.795444621429, -0.03795]
                                     ])
#
## output filepaths, if only using one fite type just make the other a
## blank string
#ZOpath = ''#'/users/bob/desktop/comparison_zeroth.std'
#FOpath = '/Users/bob/Desktop/masters_research/Analyzed_Data/P5_AA/daom_VI
                                     /daom_VIalf_first.std'
#==================================================================
```

A.4 daomaster_Data_Reducer.py

The large sections of code at the end of daomaster_Data_Reducer.py are the settings and file paths for the different data sets, to get this program to run on another computer would require extensive modifications of those file paths.

```
"""
==============================================================================

 Written by Robert Caddy.  Started on 6/16/2017, last revised 7/25/2017

 This program takes several .cor files, combines them with the data from
 the .mch, and the *all.tfr files to create a single numpy array with all
 the data for each star on each night.  It then corrects each of the
 magnitudes to the standard magnitude and saves the resulting numpy
 array using numpy

 Changelog:
     Version 1.3 - used joblib libary to parallelize reading the .cor
     files.

     Version 1.2 - Fixed a bug in daom_analyzer.Convert_Mag that didn't
     account for the comparison stars being off the frame

     Version 1.1 - Fixed bug in Stitcher that assumed that every object
     appeared in every data set.  Fixed bug in Convert_Mag that
     corrected the magnitude even if the star was missing V or I values
     in the .std file.  Now it just deletes the star.  Only applies to
     some faint stars of mag 18.8 and greater

     Version 1.0 - First version, had bugs
==============================================================================
```

```
"""

import numpy as np
import file_reader
import daom_analyzer
#import sys
from timeit import default_timer
from joblib import Parallel, delayed

start = default_timer()

####   P5_AA_VR SETTINGS
#===========================================================================
# Settings section:  Here is were we gather all the inputs and settings
# for the run including filenames, fit coefs, telescope used, etc

# a list with the path to the .cor files, make sure this is in the same
# order as the *all.mch file
corpath = ['/Users/bob/Desktop/masters_research/Analyzed_Data/P5_AA/
                                      daom_files/daom_V/daom_Valf.cor',
           '/Users/bob/Desktop/masters_research/Analyzed_Data/P5_AA/
                                                 daom_files/daom_R/
                                                 daom_Ralf.cor']

# a list with the path to the .mch files, make sure this is in the same
# order as the *all.mch file
mchpath = ['/Users/bob/Desktop/masters_research/Analyzed_Data/P5_AA/
                                      daom_files/daom_V/daom_Valf.mch',
           '/Users/bob/Desktop/masters_research/Analyzed_Data/P5_AA/
                                                 daom_files/daom_R/
                                                 daom_Ralf.mch']
```

```
# Path to the .std file with the average standard V and I
stdpath = '/Users/bob/Desktop/masters_research/Analyzed_Data/P5_AA/
                                    daom_files/daom_VR/daom_VRalf_first.
                                    std'

# Path to the .raw file for the comparison stars
compath = '/Users/bob/Desktop/masters_research/Analyzed_Data/P5_AA/
                                    comparison_VR.com'

# Path to the transfer table to correct ID numbers
tfrpath = '/Users/bob/Desktop/masters_research/Analyzed_Data/P5_AA/
                                    daom_files/daom_VR/daom_VRalf.tfr'

# Path the where you want to save the output file
savepath = '/Users/bob/scratch/P5_AA_VR.npy'

# Which Telescope was used
tele = 'P5_AA'

# Order of filters
filtorder = ['V','R']

# First order magnitude correction coefficients.  Same order as the
# *all.mch file
c1 = np.array([5.907696E-2, 9.368310E-2])

# Standard ID numbers of comparison stars, must be floats AND in the same
# order as the .com file
compID = np.array([42., 6., 16., 12., 9., 4.])
#=========================================================================
```

```
'''Controller for the entire program'''
# retrieve the data from all the .cor files.  NOTE these files do NOT use
                                        the
# standard ID's
print('\nReading .cor files')

cordata = Parallel(n_jobs=len(corpath))(delayed
                   (file_reader.Cor_Reader)(mchpath[i], corpath[i], tele)
                   for i in range(len(corpath)))

# retrieve the data from the .std file with the average standard
# magnitudes for each star.  NOTE: this file DOES use the
# standard ID numbers
stddata = file_reader.Std_Reader(stdpath, len(corpath))

# retrieve the data from the .tfr file so we can convert everything to the
# standard ID's
tfrtable = file_reader.Tfr_Reader(tfrpath, len(corpath))

# retrieve the data from comparison.com file.  NOTE this file DOES use the
# standard ID's
comdata = file_reader.Com_Reader(compath)
print('\nFinished reading all files')

# convert all the ID's in the .cor data to standard ID's using the
# tfrtable the np.delete bit feeds this function only the ID parts
# of the tfrtable
print("\nCorrecting ID's")
cordata = daom_analyzer.ID_Converter(cordata, np.delete(tfrtable,np.s_[1:3
                                        ],1))

# convert the instrumental magnitudes to standard magnitudes
```

```
# NOTE: REWRITE THIS FUNCTION IF FILTERS ARE NOT V,I,V,I...
print('\nConverting instrumental magnitudes to standard magnitudes')
cordata = daom_analyzer.Convert_Mag(cordata, comdata, stddata, compID, c1)

# convert data from each .cor file into a structured array then stitch the
# structured arrays together
print('\nStitching all the data together')
photometry = daom_analyzer.Stitcher(cordata, tfrtable, filtorder)

# save the final Photometry to a binary format
np.save(savepath,photometry)

print(f'\nTime to execute: {round(default_timer()-start,6)} seconds')



######  P1_AU Settings
##=========================================================================
## Settings section:  Here is were we gather all the inputs and settings
## for the run including filenames, fit coefs, telescope used, etc
#
## a list with the path to the .cor files, make sure this is in the same
## order as the *all.mch file
#corpath = ['/Users/bob/Desktop/masters_research/Analyzed_Data/P1_AU/
                                     daom_Vpostrot/daom_Vpostrot.cor',
#            '/Users/bob/Desktop/masters_research/Analyzed_Data/P1_AU/
                                     daom_Ipostrot/daom_Ipostrot.cor',
#            '/Users/bob/Desktop/masters_research/Analyzed_Data/P1_AU/
                                     daom_Vprerot/daom_Vprerot.cor',
#            '/Users/bob/Desktop/masters_research/Analyzed_Data/P1_AU/
                                     daom_Iprerot/daom_Iprerot.cor']
#
## a list with the path to the .mch files, make sure this is in the same
```

```
## order as the *all.mch file
#mchpath = ['/Users/bob/Desktop/masters_research/Analyzed_Data/P1_AU/
                                    daom_Vpostrot/daom_Vpostrot.mch',
#           '/Users/bob/Desktop/masters_research/Analyzed_Data/P1_AU/
                                    daom_Ipostrot/daom_Ipostrot.mch',
#           '/Users/bob/Desktop/masters_research/Analyzed_Data/P1_AU/
                                    daom_Vprerot/daom_Vprerot.mch',
#           '/Users/bob/Desktop/masters_research/Analyzed_Data/P1_AU/
                                    daom_Iprerot/daom_Iprerot.mch']
#
## Path to the .std file with the average standard V and I
#stdpath = '/Users/bob/Desktop/masters_research/Analyzed_Data/P1_AU/
                                    instru_mag_2_std_mag/daom_VIall_first
                                    .std'
#
## Path to the .raw file for the comparison stars
#compath = '/Users/bob/Desktop/masters_research/Analyzed_Data/P1_AU/
                                    comparison.com'
#
## Path to the transfer table to correct ID numbers
#tfrpath = '/Users/bob/Desktop/masters_research/Analyzed_Data/P1_AU/
                                    daom_VIall/daom_VIall.tfr'
#
## Path the where you want to save the output file
#savepath = '/users/bob/scratch/P1_AU_test3.npy'
#
## Which Telescope was used
#tele = 'P1_AU'
#
## Order of filters
#filtorder = ['V','I','V','I']
#
```

```
## First order magnitude correction coefficients.  Same order as the
## *all.mch file
#c1 = np.array([2.069024E-2,-6.617226E-3,1.352718E-2,2.403214E-3])
#
## Standard ID numbers of comparison stars, must be floats AND in
## the same order as the .com file
#compID = np.array([ 10., 22., 23., 27., 28., 36., 38., 41., 42., 50., 60
                                    ., 72., 75.,128., 165.])
##=========================================================================



#####   P5_AA_VI SETTINGS
##=========================================================================
## Settings section:  Here is were we gather all the inputs and settings
## for the run including filenames, fit coefs, telescope used, etc
#
## a list with the path to the .cor files, make sure this is in the same
## order as the *all.mch file
#corpath = ['/Users/bob/Desktop/masters_research/Analyzed_Data/P5_AA/
                                    daom_V/daom_Valf.cor',
#            '/Users/bob/Desktop/masters_research/Analyzed_Data/P5_AA/
                                    daom_I/daom_Ialf.cor']
#
## a list with the path to the .mch files, make sure this is in the same
## order as the *all.mch file
#mchpath = ['/Users/bob/Desktop/masters_research/Analyzed_Data/P5_AA/
                                    daom_V/daom_Valf.mch',
#            '/Users/bob/Desktop/masters_research/Analyzed_Data/P5_AA/
                                    daom_I/daom_Ialf.mch']
#
## Path to the .std file with the average standard V and I
#stdpath = '/Users/bob/Desktop/masters_research/Analyzed_Data/P5_AA/
```

```
                                    daom_VI/daom_VIalf_first.std'
#
## Path to the .raw file for the comparison stars
#compath = '/Users/bob/Desktop/masters_research/Analyzed_Data/P5_AA/
                                    comparison_VI.com'
#
## Path to the transfer table to correct ID numbers
#tfrpath = '/Users/bob/Desktop/masters_research/Analyzed_Data/P5_AA/
                                    daom_VI/daom_VIalf.tfr'
#
## Path the where you want to save the output file
#savepath = '/Users/bob/scratch/P5_AA_Photometry.npy'
#
## Which Telescope was used
#tele = 'P5_AA'
#
## Order of filters
#filtorder = ['V','I']
#
## First order magnitude correction coefficients.  Same order as the
## *all.mch file
#c1 = np.array([0.02406, -0.03795])
#
## Standard ID numbers of comparison stars, must be floats AND in
## the same order as the .com file
#compID = np.array([42., 6., 16., 12., 9., 21., 5., 4.])
##==========================================================================


#####   P5_AA_BR SETTINGS
##==========================================================================
## Settings section:  Here is were we gather all the inputs and settings
```

```
## for the run including filenames, fit coefs, telescope used, etc
#
## a list with the path to the .cor files, make sure this is in the same
## order as the *all.mch file
#corpath = ['/Users/bob/Desktop/masters_research/Analyzed_Data/P5_AA/
                                          daom_B/daom_Balf.cor',
#            '/Users/bob/Desktop/masters_research/Analyzed_Data/P5_AA/
                                          daom_R/daom_Ralf.cor']
#
## a list with the path to the .mch files, make sure this is in the same
## order as the *all.mch file
#mchpath = ['/Users/bob/Desktop/masters_research/Analyzed_Data/P5_AA/
                                          daom_B/daom_Balf.mch',
#            '/Users/bob/Desktop/masters_research/Analyzed_Data/P5_AA/
                                          daom_R/daom_Ralf.mch']
#
## Path to the .std file with the average standard V and I
#stdpath = '/Users/bob/Desktop/masters_research/Analyzed_Data/P5_AA/
                                          daom_BR/daom_BRalf_first.std'
#
## Path to the .raw file for the comparison stars
#compath = '/Users/bob/Desktop/masters_research/Analyzed_Data/P5_AA/
                                          comparison_BR.com'
#
## Path to the transfer table to correct ID numbers
#tfrpath = '/Users/bob/Desktop/masters_research/Analyzed_Data/P5_AA/
                                          daom_BR/daom_BRalf.tfr'
#
## Path the where you want to save the output file
#savepath = '/Users/bob/scratch/P5_AA_BR.npy'
#
## Which Telescope was used
```

```
#tele = 'P5_AA'
#
## Order of filters
#filtorder = ['B','R']
#
## First order magnitude correction coefficients.  Same order as the
##  *all.mch file
#c1 = np.array([-1.284038E-1, 2.257442E-2])
#
## Standard ID numbers of comparison stars, must be floats AND in
## the same order as the .com file
#compID = np.array([42.,  6., 16., 12.,  9.,  4.])
##=============================================================================


#####   P5_AU SETTINGS
##=============================================================================
## Settings section:  Here is were we gather all the inputs and settings
## for the run including filenames, fit coefs, telescope used, etc
#
## a list with the path to the .cor files, make sure this is in the same
## order as the *all.mch file
#corpath = ['/Users/bob/Desktop/masters_research/Analyzed_Data/P5_AU/
                                      daom_VE/daom_VE.cor',
#            '/Users/bob/Desktop/masters_research/Analyzed_Data/P5_AU/
                                      daom_IE/daom_IE.cor',
#            '/Users/bob/Desktop/masters_research/Analyzed_Data/P5_AU/
                                      daom_VL/daom_VL.cor',
#            '/Users/bob/Desktop/masters_research/Analyzed_Data/P5_AU/
                                      daom_IL/daom_IL.cor']
#
## a list with the path to the .mch files, make sure this is in the same
```

```
## order as the *all.mch file
#mchpath = ['/Users/bob/Desktop/masters_research/Analyzed_Data/P5_AU/
                                    daom_VE/daom_VE2.mch',
#            '/Users/bob/Desktop/masters_research/Analyzed_Data/P5_AU/
                                    daom_IE/daom_IE.mch',
#            '/Users/bob/Desktop/masters_research/Analyzed_Data/P5_AU/
                                    daom_VL/daom_VL2.mch',
#            '/Users/bob/Desktop/masters_research/Analyzed_Data/P5_AU/
                                    daom_IL/daom_IL.mch']
#
## Path to the .std file with the average standard V and I
#stdpath = '/Users/bob/Desktop/masters_research/Analyzed_Data/P5_AU/
                                    daom_VIall/daom_VIalf_first.std'
#
## Path to the .raw file for the comparison stars
#compath = '/Users/bob/Desktop/masters_research/Analyzed_Data/P5_AU/
                                    comparison.com'
#
## Path to the transfer table to correct ID numbers
#tfrpath = '/Users/bob/Desktop/masters_research/Analyzed_Data/P5_AU/
                                    daom_VIall/daom_VIall.tfr'
#
## Path the where you want to save the output file
#savepath = '/Users/bob/scratch/P5_AU_Photometry.npy'
#
## Which Telescope was used
#tele = 'P5_AU'
#
## Order of filters
#filtorder = ['V','I','V','I']
#
## First order magnitude correction coefficients.  Same order as the
```

```
## *all.mch file
#c1 = np.array([0.02887, -0.046463, -0.00194, 0.007273])
#
## Standard ID numbers of comparison stars, must be floats AND in
## the same order as the .com file
#compID = np.array([6., 10., 16., 18., 42.])
##=========================================================================
```

A.5 file_reader.py

```
'''
=========================================================================
 This program reads all the files that are required for
 daomaster_data_reducer to run and returns those
 files in easy to use lists or numpy arrays
=========================================================================
'''

import numpy as np
from astropy.io import fits
from astropy import time, coordinates as coord, units as u



def JD_Gather(mchpath,tele):
    '''Gather the ordered list of heliocentric julian dates'''
    rawnames = np.loadtxt(mchpath, dtype=str,usecols=(0,))

    hjds = []
    images = '/Users/bob/Desktop/masters_research/raw_data/'+tele+'/'
    for i in rawnames:
        name = str(i)[1:11]+'.fits'
```

```
        try:
            hjd = fits.open(images+name)[0].header['jd-helio']
            hjds.append(hjd)
        except KeyError: #this is only used if there was not an HJD in the
                                                        header
            jd = time.Time(fits.open(images+name)[0].header['jd'], format=
                                                        'jd')
            starpos = coord.SkyCoord("19:07:42.4", "00:02:51.0",unit=(u.
                                                        hourangle, u.deg), frame=
                                                        'icrs')
            promptpos = coord.EarthLocation(-1.235786194639,-0.
                                                        526523656536)
            times = time.Time(jd, format='jd',scale='utc', location=
                                                        promptpos)
            deltahelio = times.light_travel_time(starpos, 'heliocentric')
            hjd = (deltahelio+jd).value
            hjds.append(hjd)

    return hjds




def cor_interpreter(filespath):
    ''''Reads the .cor file and returns the header and a list of lists
    with each entry being each entry in the .cor file.  Each entry
    is of the form ID, xpos, ypos, mag, error, mag, error ...'''
    with open(filespath) as file:
        raw=file.readlines()

    header = raw[:3]
    del raw[:3]
```

```
    for i in range(len(raw)):
        raw[i] = raw[i].split()
        for j in range(len(raw[i])):
            raw[i][j] = eval(raw[i][j])

    data = []
    builder = []
    for i in raw:
        if type(i[0]) == int:
            data.append(builder)
            builder = i
        elif type(i[0]) == float:
            for j in i:
                builder.append(j)
        else:
            print('It fucked up reading the .cor file')

    data.append(builder)

    del data[0]

    return header,data



def HJDS_cor_Combiner(hjds, cordata):
    ''''Combine the HJD's with the .cor data to generate a list of lists
    with ID number, xpos, and ypos in the first sublist, and hjd-mag-error
    in following sublists'''

    data = [] #new data variable

    #interate through the hjds and cordata lists to make new data list
```

```
    for dat in cordata:
        star = [dat[:3]]



        #iterate through just the mag, error part of the list to make the
        #body
        magerr = dat[3:-2]
        for j in range(0,len(magerr),2):
            star.append([hjds[j//2],magerr[j],magerr[j+1]])

        data.append(star)

    return data

def Cor_Reader(mchpath, corpath, tele):
    ''' This function takes the path to the .mch file, path to the
    .cor file, and the telescope used and returns a 3D numpy array with
    each 2D array containing three columns with the first row being the
    ID, xpos, ypos, and the subsequent rows being the heliocentric JD,
    filter magnitude, and associated error for each star. '''

    # Get Heliocentric Julian Dates from the .mch file
    hjds = JD_Gather(mchpath, tele)

    # Get data from .cor file
    header,cordata = cor_interpreter(corpath)

    # Combine HJD's and .cor data with Combiner function
    data = np.array(HJDS_cor_Combiner(hjds,cordata))

    print('Finished reading '+corpath)
```

```
    return data


def Std_Reader(stdpath, pairnum):
    '''This function takes the path to the .std file and the number of
    different magnitude-error pairs then reads in the .std file and
    returns a numpy array where column 1 is the standard ID,
    and the subsequent columns are the magnitude-error pair in the
    same order as the *all.mch file'''

    # get a tuple with the indices of all the columns to be read
    columns = [0]
    i = 3
    while len(columns)<(2*pairnum+1):
        columns.append(i)
        i += 1
    columns = tuple(columns)

    # read in the .std file
    stddata = np.loadtxt(stdpath, skiprows=3, usecols = columns)

    return stddata


def Tfr_Reader(tfrpath, setnum):
    '''This function takes the path to the .tfr file and the number of
    different data sets that are being combined then reads in the
    data from the .tfr file and returns a numpy array with the
    transfer table.  NOTE: the table is read in as floats despite the
    fact that it is made of up ints to make it the  same as the ID's
    in the other files.  The second and third columns are the
    x and y positions respectively'''
```

```
    # figure out how many rows to skip
    skip = setnum+1

    # read in the .std file
    tfrtable = np.loadtxt(tfrpath, skiprows=skip)

    return tfrtable



def Com_Reader(compath):
    '''This function simply reads the file that has all the standard V and
    I magnitudes for the comparison stars into a numpy array then
    returns that array.  The array is in the format
    "ID, xpos, ypos, V, V_err, I, I_err, V-I"'''

    columns = (0, 3, 4, 5, 6, 7)

    comdata = np.loadtxt(compath, skiprows=2, usecols=columns)

    return comdata
```

A.6 daom_analyzer.py

```
'''
=========================================================================
This module provides all of the data analysis functions for the
daomaster_Data_Reducer program.  Documentation for what
each function does is below in the functions docstring.

Author: Robert Caddy
```

```
Date created: June 17th 2017
Version: 1.0
==========================================================================
'''

import numpy as np

def ID_Converter(cordata, tfrtable):
    ''''This function converts the IDs in the .cor files into the standard
    IDs in all the other data sets and returns the cordata in the same
    format but with corrected IDs.

    Note: the error handling is done as a result of DAOMASTER not keeping
    all the stars from every set since we set it to require that the star
    show up in at least half the data sets.  Because of this we
    effectively just delete the 1000 or so stars that are missing in each
    set. These stars should be the dimmest stars or on the edge so we
    should not be losing anything that would have been useful'''

    #first we pick out just one set of cor data to work on at a time
    newcordata = []
    for i in range(len(cordata)):
        newcor = [] # list for the cor data from each file

        #build a list of the old ID's
        keyold = []
        for k in tfrtable[:,i+1]:
            keyold.append(int(k))

        # convert from old ID's to new
        for j in range(len(cordata[i][:,0,0])):
            #this try statement is to account of DAOMASTER not keeping all
```

```
            #the stars
            try:
                #get index of new ID
                loc = keyold.index(int(cordata[i][j,0,0]))
                cordata[i][j,0,0] = tfrtable[loc,0]
                newcor.append(cordata[i][j,:,:])
            except ValueError:
                pass

        newcor = sorted(newcor, key=lambda x: int(x[0][0]))
        newcordata.append(np.array(newcor))


    return newcordata


def Convert_Mag(cordata, comdata, stddata, compID, c1):
    '''This function takes in the data from the .cor files, comparison
    stars, and average corrected magnitudes for the whole data
    set then uses that to convert the instrumental magnitude to
    standard magnitude in each case.

    NOTE:  This will need to be rewritten in the future as it assumes only
    V and I data and that they are in the order V, I, V, I...'''


    VIcomp = comdata[:,-1]

    # pick out one set of cordata at a time.  f and F are used in the
    # place of v,V and i,I to indicate a generic filter
    newcordata = []
    for i in range(len(cordata)):
```

```
# determine if it's V or I
if i&1 == 0:
    Fcomp = comdata[:,1] #for V

else:
    Fcomp = comdata[:,3] #for I

# get an array of all the instrmag for comparison stars
fcomp = np.zeros(len(compID))
for ind, compstar in enumerate(compID):
    rawcomp = cordata[i][np.where(cordata[i][:,0,0]==compstar),1:,
                                                            1]
    #eliminate large values caused by missing star in image
    fcomp[ind] = np.mean(rawcomp[rawcomp<30])



# interate through the objects in each set
objlist = []
for obj in cordata[i]:
    # approximate V-I for subject star
    stdsubj = stddata[np.where(stddata[:,0]==obj[0,0])][0]

    if i&1 == 0:
        VIsubj = stdsubj[2*i+1] - stdsubj[2*i+3]

    else:
        VIsubj = stdsubj[2*(i-1)+1] - stdsubj[2*(i-1)+3]

    # accounts for and deletes objects where we don't have a V-I
    # for the object from the .std file
    if -30<VIsubj<30:
```

```
                # iterate through magnitudes in each object
                for j in range(1,len(obj)):
                    if obj[j,1] < 90.:
                        # keep only those comparison stars that appear in
                        # that image
                        Fcompnight = Fcomp[fcomp < 30]
                        VIcompnight = VIcomp[fcomp < 30]
                        fcompnight = fcomp[fcomp < 30]

                        # compute the standard mag with respect to each
                        # comparison star
                        mags = (obj[j,1] - fcompnight) + Fcompnight
                               - c1[i]*(VIsubj-VIcompnight)
                        mean = np.mean(mags)
                        cutoff = 2*np.std(mags)
                        #eliminate high outliers
                        mags = mags[mags < (mean+cutoff)]
                        #eliminate low outliers
                        mags = mags[mags > (mean-cutoff)]
                        obj[j,1] = np.mean(mags)

                objlist.append(obj)
        newcordata.append(np.array(objlist))

    return newcordata



def Stitcher(cordata, tfrtable, filtorder):
    '''This function takes the data from cordata and creates large
    structered arrays with the form
    "HJD, V, Verr, I, Ierr, R, Rerr, B, Berr"
    and a header row with the ID, Xpos, Ypos, then zeroes.
```

```
Since a given HJD will only corrospond to a single image the
other spots are filled with None type'''

# the dtype for each column
dtypeformat = [('HJD', np.float64),
            ('V',np.float64),('Verr',np.float64),
            ('I',np.float64),('Ierr',np.float64),
            ('R',np.float64),('Rerr',np.float64),
            ('B',np.float64),('Berr',np.float64)]

# the new array that everything will be in, it's a list for now but I
# will convert it later.  Arrays don't like to be appended to
photometry = []
# iterate through all the ID's
for tfrnum in range(len(tfrtable[:,0])):
    ID=tfrtable[tfrnum,0]

    # get all the data for a given ID
    obj = []
    for cor in cordata:
        search = cor[np.where(cor[:,0,0]==ID)]
        if np.size(search) != 0:
            obj.append(search[0])
        else:
            obj.append([None])

    # make the header row, must be a tuple or the structured array
    # won't work
    header = (ID, tfrtable[tfrnum,1], tfrtable[tfrnum,2], None, None,
                                            None, None, None, None)

    # build each data row
```

```
    rows = [header]
    for i in range(len(obj)):



        if len(obj[i]) > 1: #skip empty values
            filt = filtorder[i]
            # Choose position of data based on filter

            #DAOPHOT uses 99.999 and 9.9999 as the error type for
            #missing magnitudes and errors respectively. The if
            #statements stops this function from forming rows for
            #those missing values
            if filt == 'V':
                for j in range(1,len(obj[i])):
                    if obj[i][j,1] < 90:
                        rows.append((obj[i][j,0], obj[i][j,1], obj[i][
                                                                j,2],
                                                                None,
                                                                None,
                                                                None,
                                                                None,
                                                                None,
                                                                None))
            elif filt == 'I':
                for j in range(1,len(obj[i])):
                    if obj[i][j,1] < 90:
                        rows.append((obj[i][j,0], None, None, obj[i][j
                                                                ,1], obj[
                                                                i][j,2],
                                                                None,
                                                                None,
                                                                None,
```

```
                                                      None))
            elif filt == 'R':
                for j in range(1,len(obj[i])):
                    if obj[i][j,1] < 90:
                        rows.append((obj[i][j,0], None, None, None,
                                                      None, obj
                                                      [i][j,1],
                                                       obj[i][j
                                                      ,2], None
                                                      , None))
            elif filt == 'B':
                for j in range(1,len(obj[i])):
                    if obj[i][j,1] < 90:
                        rows.append((obj[i][j,0], None, None, None,
                                                      None,
                                                      None,
                                                      None, obj
                                                      [i][j,1],
                                                       obj[i][j
                                                      ,2]))

    photometry.append(np.array(rows, dtype=dtypeformat))

return np.array(photometry)
```